Complete analytical solution to the Cornell potential and heavy quarkonium structure

M. Napsuciale[(1)], S. Rodríguez[(2)], A.E. Villanueva-Gutiérrez[(3)]

[(1)]*Departamento de Física, Universidad de Guanajuato, Lomas del Campestre 103,*
Fraccionamiento Lomas del Campestre, 37150, León, Guanajuato, México.
[(2)]*Facultad de Ciencias Físico-Matemáticas, Universidad Autónoma de Coahuila,*
Edificio A, Unidad Camporredondo, 25000, Saltillo, Coahuila, México. and
[(3)]*Escuela Superior de Física y Matemáticas, Instituto Politécnico Nacional,*
Avenida Instituto Politécnico Nacional S/N, Edificio 9,
Unidad Profesional "Adolfo López Mateos", Colonia San Pedro Zacatenco,
Delegación Gustavo A. Madero, 07700, CDMX, México

We use the recently proposed supersymmetric expansion algorithm (SEA) to obtain a complete analytical solution to the Schrödinger equation with the Cornell potential. We find that the energy levels $E_{nl}(\lambda)$ depend on n^2 and $L^2 = l(l+1)$. For a given n, the energy *decreases* with l and the radial probabilities follow the Coulomb pattern but their peaks are shifted toward smaller radius. We study the heavy quarkonium structure on the light of these results, showing that the measured $\bar{b}b$ and $\bar{c}c$ meson masses follow the inverted spectrum pattern predicted by the Cornell potential. Details of the structure of heavy quarkonium like the mean inverse radius and mean squared velocity for the different quarkonium configurations can be obtained from our solution. These details signal to significant relativistic corrections for all the configurations of real heavy quarkonium. We calculate relativistic corrections using perturbation theory finding an expansion in α_s^2 for the heavy quarkonium masses. The mass hierarchies in the fine splittings can be qualitatively understood from this expansion. The quantitative analysis of the Bohr-like levels and of the fine splittings in the $l = 0$ sector allow us to make well defined predictions for the masses of some of the missing heavy quarkonium states, to identify the $\psi(4040)$ as the 3^3S_1 $\bar{c}c$ state and to identify states that cannot be $\bar{c}c$ states in the $n = 3$ level of the measured charmonium spectrum.

I. INTRODUCTION

The Cornell potential, also named linear plus Coulomb or funnel potential in the literature, was one of the first models for the phenomenological description of the confined dynamics of quarkonium [1–3]. The potential is a sum of a Coulomb term and a linear term. The Coulomb term is motivated form the perturbative short distance regime of Quantum Chromodynamics (QCD). At intermediate and long distances (compared to the typical size of the heavy quarkonium), we face the unsolved problem of confinement.

The formal derivation of quark-antiquark forces from QCD started with the pioneering work by Wilson [4] who related the interquark potential to the so called Wilson loop. The evaluation of the Wilson loop in the long distance regime, with diverse methods, yield a linear potential as the leading term [5–12]. The physical picture that arises at long distances under reasonable assumptions is an inter-quark potential generated by a chromo-electric flux tube [8] yielding a QCD string. These results put on a firm basis the Coulomb plus linear potential as a suitable starting point for the phenomenological description of the structure of heavy quarkonium.

The systematic calculation of heavy quarkonium properties from QCD had considerable advances with the formulation of effective field theories for QCD in the non-relativistic regime. The non-relativistic expansion of QCD (NRQCD) [13] and the potential non-relativistic QCD expansion ($pNRQCD$) [14], take care of the scales of heavy quarkonium, integrate physics at high energy and yield systematic expansions in terms of operators suppressed according to the corresponding power counting rules. In the case of NRQCD there are two scales m_Q and $m_Q v^2$ with a well defined hierarchy, $m_Q >> m_Q v^2$ and the effective theory is obtained integrating out the degrees of freedom at the scale m_Q. For heavy quarkonium, a hierarchy $m_Q >> m_Q v >> m_Q v^2 >> \Lambda_{QCD}$ is expected and $pNRQCD$ obtains the effective theory for physics at the ultrasoft scale $m_Q v^2$ integrating out also physics at the soft scale $m_Q v$. A primary concern for the $pNRQCD$ is the validity of this scale hierarchy which grants the validity of the perturbative matching which otherwise must be done considering the strong coupling regime. Presently, it is not clear if all heavy quarkonium configurations respect the above hierarchy (the weak coupling scenario) or some states actually requires to work in the strong coupling matching scenario. On the other side, calculations in the lattice became efficient with the use of effective field theories and yield the same conclusion: the non-relativistic description of QCD in the non-perturbative region is given by the Cornell potential [15, 16]. A complete analytical solution to the Cornell potential is desirable because it can shed light into the structure of real heavy quarkonium, specially of the relative size of the soft and ultrasoft scales and Λ_{QCD}.

The approach followed in Refs. [1–3] and almost in every subsequent work on analytical solutions to the Cornell potential, was to consider first the linear potential whose exact solutions for S-waves are given in terms of the Airy

functions, and to incorporate later the effects of the Coulomb part using Rayleigh-Schrodinger perturbation theory to obtain approximate solutions with an expansion in powers of the strong coupling constant α_s. The lack of complete analytical solutions to the Cornell potential motivated the use of general results aiming to guess from non-relativistic quantum mechanics the structure of heavy quarkonium [17, 18], but most of the work on the field has been done using numerical solutions for the Cornell potential [19–30].

Although such solutions have been used for almost half a century to get insight on the heavy quarkonium dynamics, the relative importance of the non-perturbative effects modeled by the linear term and the perturbative effects has not been clearly stablished, precisely because the later are incorporated only in a perturbative manner. Recently, there has been renewed interest in the heavy quarkonium spectrum due to the possibilities opened by new factories for the discovery of conventional heavy quarkonium as well as exotic states (for a review on these possibilities and a more complete list of references to old literature see [31–33]).

A review and classification of the different methods aiming to obtain analytical solutions to the Schrödinger equation and a novel systematic method named Supersymmetric Expansion Algorithm (SEA) was recently published [34]. The SEA allows us to use the full power of supersymmetry in non-relativistic quantum mechanics and complete analytical solutions to long standing unsolved potentials relevant to several branches of natural sciences like the Yukawa potential [35], [36], Hulthén and anharmonic potentials [34] have been obtained by this method. In this work, we use the SEA to obtain the complete analytical solutions of the Cornell potential, apply the solutions to the description of the physics of heavy quarkonium and explore the leading relativistic corrections. We are able to extract general qualitative and quantitative predictions for the bottomonium and charmonium spectrum which nicely agree with existing data.

This paper is organized as follows. In the next section we give the detail of the calculation of the complete analytical solution for the Cornell potential. Section III is devoted to the calculation of the heavy quarkonium spectrum using the solutions to the Cornell potential and its comparison with existing data. In section IV we consider the leading relativistic corrections that yield the fine splittings. Section V is devoted to a first quantitative analysis of the fine splittings in the $l = 0$ sector, qualitative analysis of the fine splittings for $l = 1, 2$ and the corresponding quantitative and qualitative predictions for the bottomonium and charmonium spectrum. We close with our conclusions and perspectives in section VI.

II. THE CORNELL POTENTIAL IN THE SEA

The Cornell potential is given by

$$V_c(r) = -\frac{\alpha \hbar c}{r} + \frac{\sigma}{\hbar c} r. \tag{1}$$

We introduce in this section the $\hbar$ and c factor in order to have a dimensionless parameter α and a parameter σ with units of E^2. In the remaining of this section we will solve the Schrödinger equation (SE) for the linear plus Coulomb potential using the supersymmetric expansion algorithm introduced in Ref. [34]. We refer the reader to that work for further details of the formalism. In a first step, we use the typical distance scale of the system as the scale related to the coupling α, $i.e.$ the Bohr radius

$$a = \hbar/\mu c \alpha, \tag{2}$$

where μ is the reduced mass of the system, to cast the radial part of the Schrödinger equation into its dimensionless form

$$\left[-\frac{d^2}{dx^2} + v_0(x, \lambda) \right] u_0(x, \lambda) = \epsilon_0(\lambda) u_0(x, \lambda), \tag{3}$$

where a suffix "0" is attached to all quantities because this is the initial step of the algorithm. Here, $x = r/a$, $R(r) = u_0(x)/x$, $\epsilon_0(\lambda) = E_0(\lambda)/E_c$, with the typical energy scale given by the Coulomb energy $E_c = \hbar^2/2\mu a^2 = \mu c^2 \alpha^2/2$. The dimensionless effective potential for the Cornell potential is given by

$$v_0(x, \lambda) = \frac{l(l+1)}{x^2} - \frac{2}{x} + \lambda x, \tag{4}$$

with the normalized string tension

$$\lambda = \frac{\sigma}{E_c E_s} = \frac{2\sigma}{(\mu c^2)^2 \alpha^3}, \tag{5}$$

where $E_s = \hbar c/a = \mu c^2 \alpha$.

The SEA construct the complete analytical solution starting with very special states named edge states, which in general are nodeless (excited or ground) states. With this aim, we first recast the SE into a logarithmic form

$$W_0^2(x, \lambda) - W_0' = v_0(x, \lambda) - \epsilon_0(\lambda). \tag{6}$$

where

$$W_0(x, \lambda) = -\frac{d}{dx} \ln u_0(x, \lambda). \tag{7}$$

The solution to equation (6) is obtained as power series in λ

$$v_0(x, \lambda) = \sum_{k=0}^{\infty} v_{0k}(x)\lambda^k, \qquad W_0(x, \lambda) = \sum_{k=0}^{\infty} w_{0k}(x)\lambda^k, \qquad \epsilon_0(\lambda) = \sum_{k=0}^{\infty} \varepsilon_{0k}\lambda^k. \tag{8}$$

The coefficients for the expansion of the Cornell potential in powers of λ are given by

$$v_{0k}(x) = \begin{cases} \frac{l(l+1)}{x^2} - \frac{2}{x} & for \quad k = 0, \\ x & for \quad k = 1, \\ 0 & for \quad k \geq 2. \end{cases} \tag{9}$$

The coefficients in the power series of $W_0(x, \lambda)$ and $\epsilon_0(\lambda)$ satisfy the following infinite set of hierarchical equations

$$k = 0: \qquad w_{00}^2 - w_{00}' = \frac{l(l+1)}{x^2} - \frac{2}{x} - \varepsilon_{00}, \tag{10}$$

$$k = 1: \qquad 2w_{00}w_{01} - w_{01}' = x - \varepsilon_{01} \tag{11}$$

$$k \geq 2: \qquad 2w_{00}w_{0k} - w_{0k}' = -B_{0k}(x) - \varepsilon_{0k}, \tag{12}$$

where

$$B_{0k} = \sum_{m+n=k} w_{0m}w_{0n}. \tag{13}$$

The solutions up to $k = 5$ are given by

$$w_{00} = \frac{1}{b} - \frac{b}{x}, \tag{14}$$

$$w_{01} = \frac{b}{2}x, \tag{15}$$

$$w_{02} = -\frac{b^3}{8} \left[b(b+1)x + x^2 \right], \tag{16}$$

$$w_{03} = \frac{b^5}{32} \left[b^2(b+1)(4b+5)x + b(4b+5)x^2 + 2x^3 \right], \tag{17}$$

$$w_{04} = -\frac{b^7}{256} \left[b^3(b+1)(48b^2 + 129b + 88)x + b^2(48b^2 + 129b + 88)x^2 + 2b(15b+22)x^3 + 10x^4 \right], \tag{18}$$

$$w_{05} = \frac{b^9}{512} \left[b^4(b+1)(176b^3 + 753b^2 + 1049b + 539)x + b^3(176b^3 + 753b^2 + 1049b + 539)x^2 \right.$$
$$\left. + 2b^2(60b^2 + 185b + 147)x^3 + b(56b+93)x^4 + 14x^5 \right], \tag{19}$$

$$\varepsilon_{00} = -\frac{1}{b^2}, \tag{20}$$

$$\varepsilon_{01} = \frac{b}{2}(2b+1), \tag{21}$$

$$\varepsilon_{02} = -\frac{b^4}{8}(b+1)(2b+1), \tag{22}$$

$$\varepsilon_{03} = \frac{b^7}{32}(b+1)(2b+1)(4b+5), \tag{23}$$

$$\varepsilon_{04} = -\frac{b^{10}}{256}(b+1)(2b+1)(48b^2 + 129b + 88), \tag{24}$$

$$\varepsilon_{05} = \frac{b^{13}}{512}(b+1)(2b+1)(176b^3 + 753b^2 + 1049b + 539), \tag{25}$$

where

$$b = l + 1. \tag{26}$$

In general, for $k \geq 2$ we have polynomial solutions for $w_{0k}(x)$

$$w_{0k}(x) = \sum_{\alpha=1}^{k} w_{0k\alpha} x^{\alpha} \tag{27}$$

and inserting this expression in Eqs. (12) we get the following recursion relations for the constant coefficients $w_{0k\alpha}$

$$w_{0kk} = -\frac{b}{2} B_{0kk}, \tag{28}$$

$$w_{0k\alpha} = \frac{b}{2} \left((2b + \alpha + 1) w_{0k(\alpha+1)} - B_{0k\alpha} \right) \qquad \alpha = k-1, k-2, ...3, 2, \tag{29}$$

$$\varepsilon_{0k} = (2b + 1) w_{0k1}, \tag{30}$$

where

$$B_{0k\alpha} = \sum_{m+n=k} \sum_{\beta+\gamma=\alpha} w_{0m\beta} w_{0n\gamma}. \tag{31}$$

These recurrence relations yields the first solution for the Cornell Hamiltonian

$$H_0 = -\frac{d^2}{dx^2} + v_0(x, \lambda). \tag{32}$$

Indeed, separating the λ-independent terms

$$W_0(x, \lambda) = \frac{1}{l+1} - \frac{l+1}{x} + \sum_{k=1}^{\infty} w_{0k}(x) \lambda^k, \tag{33}$$

we can see that the λ-independent terms corresponds to the solution to the Coulomb problem, thus, for this solution, $l + 1 = n$ and skipping normalization factors we get

$$u_0(x, \lambda) = x^n e^{-\frac{x}{n}} e^{-G_0(x,\lambda)} \equiv \phi_{n,n-1}^{(0)}(x, \lambda), \tag{34}$$

$$\epsilon_0(\lambda) = -\frac{1}{n^2} + \sum_{k=1}^{\infty} (2n + 1) w_{0k1} \lambda^k, \tag{35}$$

where we used $\phi_{nl}^{(0)}(x, \lambda)$ for the solutions with the principal quantum number n and angular momentum l of the Cornell Hamiltonian H_0. The function G_0 is given by

$$G_0(x, \lambda) = \sum_{k=1}^{\infty} \lambda^k \left(\sum_{\alpha=1}^{k} w_{0k\alpha} \frac{x^{\alpha+1}}{\alpha+1} \right). \tag{36}$$

The solution $\phi_{n,n-1}^{(0)}(x, \lambda)$ is the edge state for the n-level of the Cornel Hamiltonian H_0. The rest of the states in this level are constructed with the aid of supersymmetry. We start noticing that H_0 can be be factorized as

$$H_0 = a_0^\dagger a_0 + \epsilon_0, \tag{37}$$

where

$$a_0 = \frac{d}{dx} + W_0, \qquad a_0^\dagger = -\frac{d}{dx} + W_0. \tag{38}$$

and the edge state u_0 satisfies

$$a_0 u_0(x, \lambda) = 0. \tag{39}$$

Then we construct the supersymmetric partner

$$H_1 = a_0 a_0^\dagger + \epsilon_0 = -\frac{d^2}{dx^2} + v_1(x, \lambda), \tag{40}$$

with

$$v_1(x, \lambda) = v_0(x, \lambda) + 2W_0' = \frac{l(l+1)}{x^2} - \frac{2}{x} + \lambda x + 2\sum_{k=0}^{\infty} w_{0k}'(x)\lambda^k. \tag{41}$$

Now we find the edge state solution for H_1 in a similar way as we did it for H_0, i.e., we recast the Schrödinger equation for H_1 in the logarithmic form

$$W_1^2 - W_1' = v_1(x, \lambda) - \epsilon_1(\lambda) = v_0(x, \lambda) + 2W_0' - \epsilon_1(\lambda), \tag{42}$$

where

$$W_1(x, \lambda) = -\frac{d}{dx} \ln u_1(x, \lambda). \tag{43}$$

The solution to equation (42) is obtained as power series in λ

$$v_1(x, \lambda) = \sum_{k=0}^{\infty} v_{1k}(x)\lambda^k, \qquad W_1(x, \lambda) = \sum_{k=1}^{\infty} w_{1k}(x)\lambda^k, \qquad \epsilon_1(\lambda) = \sum_{k=1}^{\infty} \varepsilon_{1k}\lambda^k. \tag{44}$$

The coefficients for the expansion of v_1 in powers of λ are given by

$$v_{1k}(x) = \begin{cases} \frac{l(l+1)}{x^2} - \frac{2}{x} + 2w_{00}' & for \quad k = 0, \\ x + 2w_{01}' & for \quad k = 1, \\ 2w_{0k}' & for \quad k \geq 2. \end{cases} \tag{45}$$

The coefficients in the power series of $W_1(x, \lambda)$ and $\epsilon_1(\lambda)$ satisfy now the following infinite set of hierarchical equations

$$k = 0: \qquad w_{10}^2 - w_{10}' = \frac{(l+1)(l+2)}{x^2} - \frac{2}{x} - \varepsilon_{10}, \tag{46}$$

$$k = 1: \qquad 2w_{10}w_{11} - w_{11}' = x + 2w_{01}' - \varepsilon_{11}, \tag{47}$$

$$k \geq 2: \qquad 2w_{10}w_{1k} - w_{1k}' = 2w_{0k}' - B_{1k} - \varepsilon_{1k}, \tag{48}$$

where

$$B_{1k} = \sum_{m+n=k} w_{1m}w_{1n}. \tag{49}$$

The solutions for $k = 0, 1$ are

$$w_{10} = \frac{1}{b+1} - \frac{b+1}{x}, \qquad\qquad \varepsilon_{10} = -\frac{1}{(b+1)^2}, \tag{50}$$

$$w_{11} = \frac{b+1}{2}x, \qquad\qquad \varepsilon_{11} = \frac{1}{2}(3(b+1)^2 - b(b-1)), \tag{51}$$

while for $k \geq 2$, w_{1k} has the general form

$$w_{1k}(x) = \sum_{\alpha=1}^{k} w_{1k\alpha}x^\alpha, \tag{52}$$

where the numerical coefficients satisfy the following recurrence relations

$$w_{1kk} = -\frac{b+1}{2}B_{1kk}, \tag{53}$$

$$w_{1k\alpha} = \frac{b+1}{2}\left((2b+3+\alpha)w_{0k(\alpha+1)} - B_{1k\alpha}\right) \qquad \alpha = k-1, k-2, ...3, 2, \tag{54}$$

$$\varepsilon_{1k} = (2b+3)w_{1k1} + 2w_{0k1}. \tag{55}$$

From the λ-independent part of the solution we identify this solution as a $l = n - 2$ solution of the level n of H_1. Explicitly, the unnormalized solution is given by

$$u_1(x, \lambda) = x^n e^{-\frac{x}{n}} e^{-G_1(x,\lambda)} \equiv \phi^{(1)}_{n,n-2}(x, \lambda), \tag{56}$$

$$\epsilon_1(\lambda) = -\frac{1}{n^2} + \sum_{k=1}^{\infty} \left((2b+3)w_{1k1} + 2w_{0k1}\right) \lambda^k. \tag{57}$$

The function G_1 is given by

$$G_1(x, \lambda) = \sum_{k=1}^{\infty} \lambda^k \left(\sum_{\alpha=1}^{k} w_{1k\alpha} \frac{x^{\alpha+1}}{\alpha+1} \right). \tag{58}$$

Supersymmetry allows us to obtain a second solution to the Cornel Hamiltonian H_0, from the edge eigenstate u_1 of H_1. Indeed, u_1 satisfies

$$H_1 u_1(x, \lambda) = [a_0 a_0^\dagger + \epsilon_0]u_1(x, \lambda) = \epsilon_1(\lambda)u_1(x, \lambda). \tag{59}$$

Acting with $a_0^\dagger$ on this equation we get

$$[a_0^\dagger a_0 + \epsilon_0]a_0^\dagger u_1(x, \lambda) = H_0 a_0^\dagger u_1(x, \lambda) = \epsilon_1(\lambda)a_0^\dagger(\lambda)u_1(x, \lambda), \tag{60}$$

thus, $a_0^\dagger u_1(x, \lambda)$ is also an eigenstate of H_0 with eigenvalue $\epsilon_1(\lambda)$. This is also a solution for the n level but now with $l = n - 2$. The unnormalized solution for H_0 is

$$\phi^{(0)}_{n,n-2}(x, \lambda) = a_0^\dagger u_1(x, \lambda) = a_0^\dagger \phi^{(1)}_{n,n-2}(x, \lambda). \tag{61}$$

Notice that in the usual nl notation, $\epsilon_1(\lambda) = \epsilon_{n,n-2}(\lambda)$, $\epsilon_0(\lambda) = \epsilon_{n,n-1}(\lambda)$ and $\epsilon_{n,n-1}(\lambda) \neq \epsilon_{n,n-2}(\lambda)$ thus de l-degeneracy of the n-th level of the Coulomb potential is broken by the linear term in the Cornell Hamiltonian H_0.

We continue this process and construct a new solution to the n-th level of H_0 factorizing now H_1 as

$$H_1 = a_1^\dagger a_1 + \epsilon_1(\lambda) \tag{62}$$

with

$$a_1 = -\frac{d}{dx} + W_1(x, \lambda), \qquad a_1^\dagger = \frac{d}{dx} + W_1(x, \lambda) \tag{63}$$

and constructing a superpartner to H_1 defined as

$$H_2 = a_1 a_1^\dagger + \epsilon_1(\lambda) = -\frac{d^2}{dx^2} + v_2(x, \lambda), \tag{64}$$

where

$$v_2(x, \lambda) = v_1(x, \lambda) + 2W_1'. \tag{65}$$

We solve likewise this potential obtaining the unnormalized solution of H_0 as

$$\phi^{(0)}_{n,n-3}(x, \lambda) = a_1^\dagger a_0^\dagger u_2(x, \lambda) = a_1^\dagger a_0^\dagger \phi^{(2)}_{n,n-3}(x, \lambda), \tag{66}$$

where $u_2(x, \lambda)$ is the solution to H_2 with eigenvalue $\epsilon_2(\lambda)$ which is a common eigenvalue of H_2, H_1, H_0.

Repeating the algorithm, in the step r we solve the r-th superpartner H_r in the same manner. The solutions for $k = 0, 1$ in this step are

$$w_{r0} = \frac{1}{b+r} - \frac{b+r}{x}, \qquad\qquad \varepsilon_{r0} = -\frac{1}{(b+r)^2}, \tag{67}$$

$$w_{r1} = \frac{b+r}{2}x, \qquad\qquad \varepsilon_{r1} = \frac{1}{2}(3(b+r)^2 - b(b-1)), \tag{68}$$

while for $k \geq 2$ the coefficients in the expansion of the r-th superpotential W_r has the general form

$$w_{rk}(x) = \sum_{\alpha=1}^{k} w_{rk\alpha} x^{\alpha}, \tag{69}$$

where the numerical coefficients satisfy the following recurrence relations

$$w_{rkk} = -\frac{b+r}{2} B_{rkk}, \tag{70}$$

$$w_{rk\alpha} = \frac{b+r}{2} \left((2b + 2r + \alpha + 1) w_{0k(\alpha+1)} + 2(\alpha+1) \sum_{q=0}^{r-1} w_{qk(\alpha+1)} - B_{rk\alpha} \right) \qquad \alpha = k-1, k-2, ...3, 2, \tag{71}$$

$$\varepsilon_{rk} = (2b + 2r + 1) w_{rk1} + 2 \sum_{q=0}^{r-1} w_{qk1}, \tag{72}$$

with

$$B_{rk\alpha} = \sum_{m+n=k} \sum_{\beta+\gamma=\alpha} w_{rm\beta} w_{rn\gamma}. \tag{73}$$

The unnormalized solution for the edge state of H_r, is given by

$$u_r(x, \lambda) = x^n e^{-\frac{x}{n}} e^{-G_r(x,\lambda)}, \tag{74}$$

$$\epsilon_r(\lambda) = \sum_{\lambda=0}^{\infty} (2n+1) w_{rk1} + 2 \sum_{q=0}^{r-1} w_{qk1}, \tag{75}$$

where

$$G_r(x, \lambda) = \int w_r(x, \lambda) dx = \sum_{k=1}^{\infty} \lambda^k \left(\sum_{\alpha=1}^{k} w_{rk\alpha} \frac{x^{\alpha+1}}{\alpha+1} \right). \tag{76}$$

The solution for the Cornell Hamiltonian H_0 in the nl notation is given by

$$\phi_{n,n-1-r}^{(0)} = a_0^\dagger a_1^\dagger ... a_{r-2}^\dagger a_{r-1}^\dagger u_r, \tag{77}$$

$$\epsilon_{n,n-1-r}(\lambda) = \sum_{\lambda=0}^{\infty} (2n+1) w_{rk1} + 2 \sum_{q=0}^{r-1} w_{qk1}. \tag{78}$$

The process terminates for $r = n - 1$ when we reach the lowest value $l = 0$ and the level n is completely solved. Notice that we started with an arbitrary value of n thus, all the levels of the Cornell potential can be solved with the supersymmetric expansion algorithm. All the information of the analytic solution resides in the coefficients of the expansion in Eq. (69) which satisfy the algebraic recurrence relations in Eq. (70,71,72). We wrote a symbolic code to solve these relations to the desired order in λ.

We find that the energy levels $\epsilon_{nl}(\lambda)$ can be written as

$$\epsilon_{nl}(\lambda) = \sum_{k=0}^{\infty} \varepsilon_k(n^2, L^2) \lambda^k \tag{79}$$

where the coefficients ε_k depend on n^2 and $L^2 = l(l+1)$. The coefficients for large k have long expressions thus we

explicitly write them only up to $k = 10$ for future reference

$$\varepsilon_0(n^2, L^2) = -\frac{1}{n^2}, \tag{80}$$

$$\varepsilon_1(n^2, L^2) = \frac{1}{2}(3n^2 - L^2), \tag{81}$$

$$\varepsilon_2(n^2, L^2) = -\frac{n^2}{16}(7n^4 - 3L^4 + 5n^2), \tag{82}$$

$$\varepsilon_3(n^2, L^2) = \frac{n^4}{64}(33n^6 - 7n^2L^4 - 10L^6 + 75n^4), \tag{83}$$

$$\varepsilon_4(n^2, L^2) = -\frac{n^6}{512}(465n^8 - 99n^4L^4 - 90n^2L^6 - 84L^8 + 2275n^6 - 180n^2L^4 + 440n^4), \tag{84}$$

$$\varepsilon_5(n^2, L^2) = \frac{n^8}{1024}\left(1995n^{10} + 17340n^8 - 3n^6\left(155L^4 - 3803\right) - 91n^4L^4\left(4L^2 + 23\right)\right.$$
$$\left. - 88n^2L^6\left(3L^2 + 10\right) - 198L^{10}\right), \tag{85}$$

$$\varepsilon_6(n^2, L^2) = -\frac{n^{10}}{16385}\left(77027n^{12} + 1060290n^{10} - 133n^8\left(150L^4 - 11663\right)\right.$$
$$- 34n^6\left(426L^6 + 4887L^4 - 5000\right) - 15n^4L^4\left(607L^4 + 5612L^2 + 4800\right)$$
$$\left. - 364n^2L^8\left(17L^2 + 75\right) - 4004L^{12}\right), \tag{86}$$

$$\varepsilon_7(n^2, L^2) = \frac{n^{12}}{131072}\left(1608201n^{14} + 32473350n^{12} - 69n^{10}\left(6698L^4 - 1254497\right)\right.$$
$$- 66n^8\left(4858L^6 + 93961L^4 - 485630\right) - 19n^6L^4(9525L^4 + 175460L^2 + 402116)$$
$$\left. - 204n^4L^6\left(543L^4 + 6378L^2 + 10000\right) - 24480n^2L^{10}\left(3L^2 + 16\right) - 66432L^{14}\right), \tag{87}$$

$$\varepsilon_8(n^2, L^2) = -\frac{n^{14}}{2097152}\left(71016319n^{16} + 1991448850n^{14} - 1323n^{12}\left(17018L^4 - 6494305\right)\right.$$
$$+ 650n^{10}\left(10847042 - 687771L^4 - 23310L^6\right)$$
$$- 69n^8\left(112885L^8 + 3576100L^6 + 15774908L^4 - 8000000\right)$$
$$- 924n^6L^4\left(4637L^6 + 106904L^4 + 443260L^2 + 264000\right)$$
$$\left. - 21280n^4L^8\left(127L^4 + 1726L^2 + 3900\right) - 31008n^2L^{12}\left(57L^2 + 350\right) - 930240L^{16}\right), \tag{88}$$

$$\varepsilon_9(n^2, L^2) = \frac{n^{16}}{4194304}\left(408787995n^{18} + 15278638650n^{16} - 341n^{14}\left(416518L^4 - 289086315\right)\right.$$
$$- 290n^{12}\left(322478L^6 + 13572891L^4 - 508132290\right)$$
$$- 9n^{10}\left(4892853L^8 + 244792100L^6 + 1786929620L^4 - 4297880080\right)$$
$$- 1300n^8L^4\left(16555L^6 + 663164L^4 + 5343868L^2 + 8175108\right)$$
$$- 184n^6L^6\left(68435L^6 + 1771020L^4 + 10489824L^2 + 12000000\right)$$
$$\left. - 170016n^4L^{10}\left(2160 + 733L^2 + 49L^4\right) - 769120n^2L^{14}\left(7L^2 + 48\right) - 2615008L^{18}\right), \tag{89}$$

$$\varepsilon_{10}(n^2, L^2) = -\frac{n^{18}}{33554432}\left(9724330239n^{20} + 469170488020n^{18}\right.$$
$$- 21n^{16}\left(175194855L^4 - 203670581987\right) - 1122n^{14}\left(2123874L^6 + 121493988L^4 - 9238989815\right)$$
$$- 1023n^{12}\left(1005969L^8 + 75201300L^6 + 829658295L^4 - 5866391024\right)$$
$$- 116n^{10}\left(3765438L^{10} + 248096745L^8 + 3398870376L^6 + 9733541337L^4 - 3239200000\right)$$
$$- 27n^8L^4\left(8514023L^8 + 379043252L^6 + 4451273932L^4 + 13108880480L^2 + 6339200000\right)$$
$$- 2340n^6L^8\left(63925L^6 + 1738820L^4 + 13359364L^2 + 23240000\right)$$
$$\left. - 215280n^4L^{12}\left(483L^4 + 7716L^2 + 28000\right) - 33153120n^2L^{16}\left(2L^2 + 15\right) - 29995680L^{20}\right). \tag{90}$$

The dependence on λ of the ground state energy is shown in Fig. (1) for calculations up to λ^k with $k = 3, 6, 9$. Clearly, the series for the energy levels have small convergence radius. However, the $\epsilon_{nl}(\lambda)$ function can be reconstructed from its Taylor series using Padé approximants $[M/N](\lambda)$. The actual value of the function lies between the $[N/N](\lambda)$ and the $[(N + 1)/N](\lambda)$. We can use this result to estimate the uncertainty in the reconstruction which is
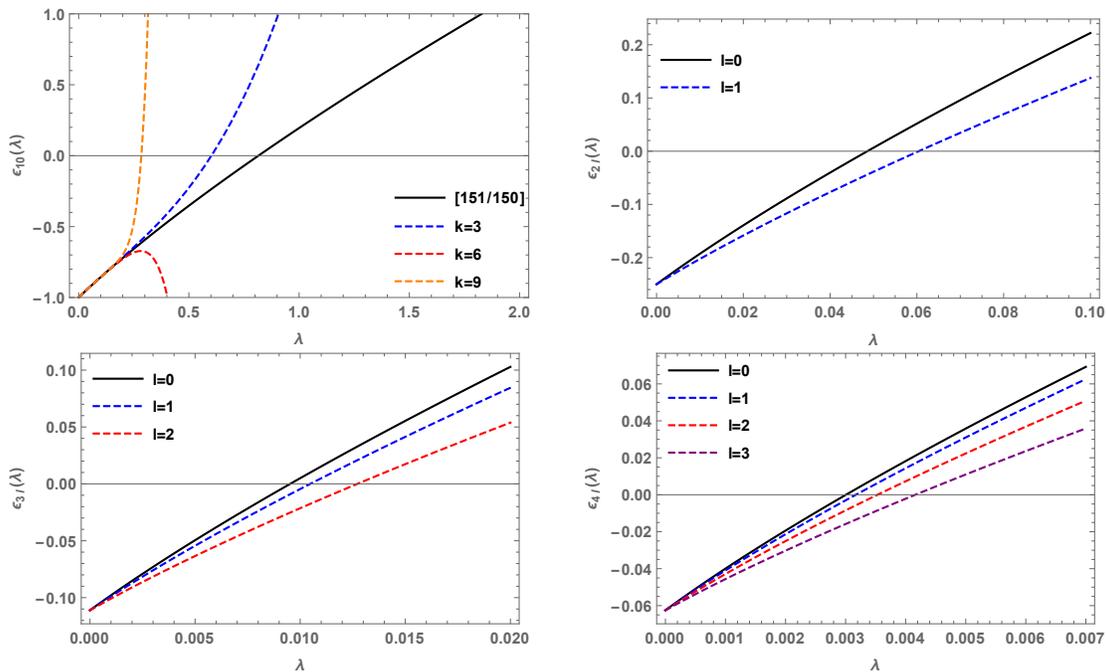
FIG. 1: Energy dependence on λ of the lowest energy levels of the Cornell potential reconstructed with the $[151/150](\lambda)$ Padé approximant. For the ground states we also show results for the series calculated up to $\mathcal{O}(\lambda^k)$ for $k = 3, 6, 9$. Notice that ϵ_{nl} *decreases* with l.

specially important for large values of λ. Unless stated explicitly, in the following we will use the reconstruction of the energy levels with $N = 150$, which requires a calculation of the corresponding series to order λ^{301}. This yields a confident reconstruction of the energy levels, for very large values of λ. The reconstructed energy functions up to $n = 4$ are also shown in Fig. (1). Notice that, in contrast to screening non-confining potentials like the Yukawa and Hulthén's potentials, in the case of the Cornell potential, for a given n, *the energy $\epsilon_{nl}(\lambda)$ decreases with l*. This is a surprising result product of the confining linear term in the potential.

A reference point for large values of λ is the critical value λ_{cr} defined by $\epsilon(\lambda_{cr}) = 0$. Unlike the Yukawa and Hulthén potentials, this is not a ionization point because we still have bound states above this critical value for the Cornell potential. In Table I we show the results for the critical values of λ for the lowest nl levels as calculated with $N = 5$. The quoted uncertainties correspond to the difference between the $[(N + 1)/N]$ and $[N/N]$ Padé approximants.

Our complete solution allows us to study also the radial probabilities for every state. Similarly to the energies, the eigenstates are convergent only for small values of λ but they can be reconstructed from the series in λ using the Padé approximants. In this case the reconstruction is more resources demanding. In Fig. (2) we plot the probabilities for the lowest lying states reconstructed with the $[5/5]$ Padé approximant, for λ close to the critical value in each case, together with the result for the Coulomb-like case corresponding to $\lambda = 0$. We can see in these plots the second surprising result in the solutions: *Radial probabilities have the same form as the Coulomb-like probabilities, the main peaks grow with n, but are shifted to smaller radius by the linear term*. Instead of the conventional delocalization of states produced by non-confining screening potential, the confining Cornell potential produces more compact states as we increase the value of λ. It is interesting that the complete solution to the Cornell potential reveals that even for values of λ as large as the critical values, the shifts are however small and the peaks remain close to the Coulomb-like values. However, in practical applications of these results it will be important to asses if the physical values of λ are around the critical values or not. We will show in the next section that for heavy quarkonium applications, except for the ground state, the physical value of λ is much larger than its critical value.

Another interesting result arising in the complete analytical solution of the non-confining screening Yukawa and Hulthén potentials in Refs. [34–36], is the phenomena of crossing of energy levels. For the Yukawa potential this phenomena starts for $n = 4$ where, for specific values of the screening parameter close to the critical values, it happens that $\epsilon_{43} \geq \epsilon_{50}$. It is interesting to study if a similar effect exists for the Cornell potential. The energy levels for the Cornell potential are shown in Fig. (3) for $n = 1, 2, 3, 4$. We find that the crossing phenomena for the Cornell potential starts with the $\epsilon_{43}(\lambda)$ level which for $\lambda \approx 0.4$ crosses with the $\epsilon_{30}(\lambda)$.

n	l	λ_{cr}
1	0	0.8157(7)
2	0	0.048585(5)
2	1	0.06042(2)
3	0	0.0095239(5)
3	1	0.0104780(8)
3	2	0.0127192(5)
4	0	0.0030054(1)
4	1	0.0031703(1)
4	2	0.0035308(3)
4	3	0.0041608(5)
5	0	0.00122952(2)
5	1	0.00127220(3)
5	2	0.00136244(5)
5	3	0.0015114(1)
5	4	0.0017395(2)

n	l	λ_c
6	0	0.00059256(1)
6	1	0.00060674(1)
6	2	0.00063623(1)
6	3	0.00068347(2)
6	4	0.00075267(4)
6	5	0.0008506(1)
7	0	0.000319724(4)
7	1	0.000325324(5)
7	2	0.000336847(6)
7	3	0.00035498(1)
7	4	0.00038086(1)
7	5	0.00041625(2)
7	6	0.00046379(3)

n	l	λ_c
8	0	0.000187368(2)
8	1	0.000189875(2)
8	2	0.000194997(3)
8	3	0.000202966(4)
8	4	0.000214156(5)
8	5	0.00022912(1)
8	6	0.000248667(1)
8	7	0.00027394(2)
9	0	0.000116953(1)
9	1	0.000118186(1)
9	2	0.000120696(2))
9	3	0.000124572(2)
9	4	0.000129955(4)
9	5	0.000137047(3)
9	6	0.000146139(5)
9	7	0.00015762(1)
9	8	0.00017204(1)

TABLE I: Critical values of λ for the Cornell potential, calculated using the reconstructed functions $\epsilon_{nl}(\lambda)$.
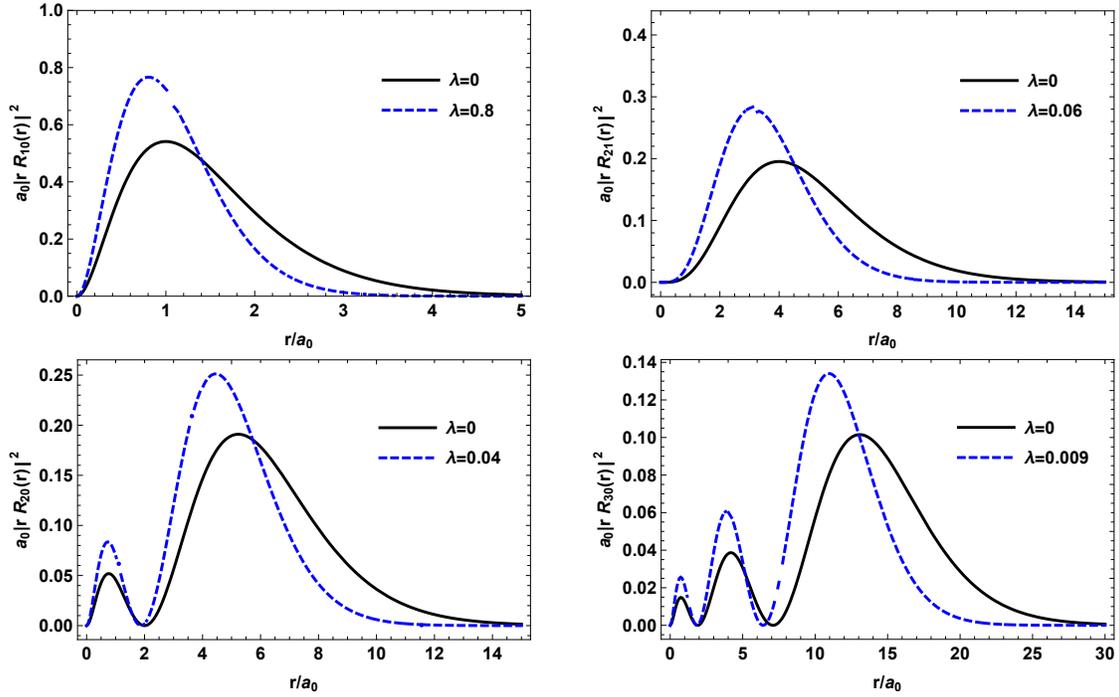
FIG. 2: Reconstruction of the probabilities for the lowest lying states of the Cornell potential with the $[5/5](\lambda)$ Padé approximant, for values of λ close to the critical values for each state and comparison with the Coulomb-like states ($\lambda = 0$).

III. STRUCTURE OF HEAVY QUARKONIUM FROM THE CORNELL POTENTIAL

There are many remarkable qualitative and quantitative conclusions that can be drawn on the heavy quarkonium systems from the analytical solutions obtained in the previous section. When applied to heavy quarkonium, the solutions for the energy, $E_{nl}(\lambda)$, yield the analogous of the Bohr levels of the hydrogen atom. There are striking differences however, starting from the fact that non-perturbative strong interactions mimicked by the linear coupling breaks the l-degeneracy of the energy levels for a given n and produces the inverted spectrum described in the previous
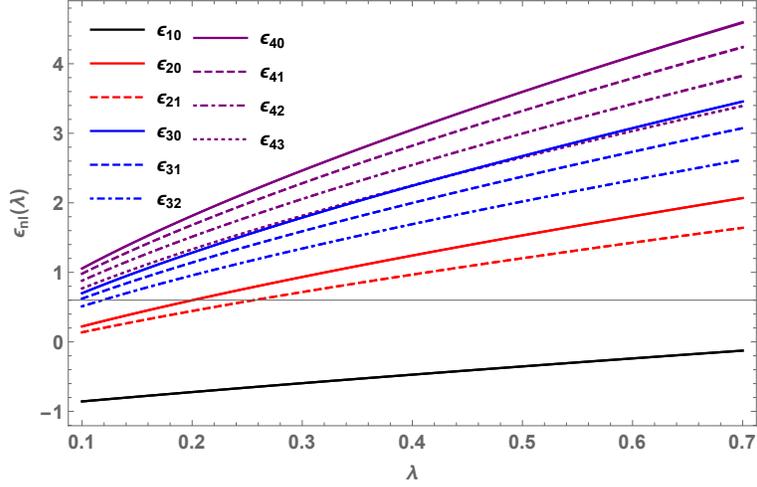
FIG. 3: Energy levels, $\epsilon_{nl}(\lambda)$, of the Cornell potential for $n = 1, 2, 3, 4$. For $\lambda \approx 0.4$ the $\epsilon_{43}(\lambda)$ level crosses with the $\epsilon_{30}(\lambda)$ level.

section.

In this section we address the predictions of our complete solution to the Cornell potential for the heavy quarkonium structure. In the following we will use the high energy physics customary natural units, i.e., we will set $\hbar = c = 1$. We start with the typical distance scale associated to the strong coupling constant. For heavy quarkonium physics, the parameter α is related to the QCD coupling α_s as

$$\alpha = \frac{4}{3}\alpha_s. \tag{91}$$

The QCD Bohr radius arising from this coupling constant and denoted in the following as a_Q, is the typical length scale for quarkonium and considering Eq. (91) and the fact that for heavy quarkonium the reduced mass is $\mu = m_Q/2$ we get

$$a_Q = \frac{3}{2}\frac{1}{m_Q\alpha_s(m_Q)}. \tag{92}$$

For heavy quarkonium, the dimensionless coupling λ in Eq. (5) is related to the QCD coupling constant α_s and the string tension σ as

$$\lambda = \frac{27}{8}\frac{\sigma}{m_Q^2\alpha_s^3}. \tag{93}$$

The masses of heavy quarkonium states can be written to leading order in a non-relativistic expansion in terms of the eigenvalues of the Cornell potential as

$$M(n^{2S+1}L_J)(m_Q, \alpha_s(m_Q), \lambda_Q) = 2m_Q + \frac{4}{9}m_Q\alpha_s^2(m_Q)\epsilon_{nl}(\lambda_Q), \tag{94}$$

where $m_Q, \alpha_s(m_Q)$ and λ_Q denote the physical values of the corresponding quantities for the heavy quark Q. Notice that for $\lambda = 0$ the energy levels reduce to the Coulomb values $\epsilon_{nl}(0) = -1/n^2$. Our solution allows to go in a controlled manner from the perturbative Coulomb values to the non-perturbative region mimicked by non-zero values of the normalized string tension λ.

We remark that we have two well defined scales in Eq. (94)

$$\mu_Q(m_Q) = 2m_Q, \tag{95}$$

$$\mu_B(m_Q) = \frac{4}{9}m_Q\alpha_s^2(m_Q). \tag{96}$$

The scale μ_Q is the scale of the perturbative effects while $\mu_B(m_Q)$ corresponds to the reference energy scale for the Bohr-like levels of heavy quarkonium.

The outstanding result of our complete analytical solution to the Cornell potential is the inverted spectrum, i.e. a spectrum where, for a given n, states with higher values of l have a lower mass. This pattern is counter-intuitive on the light of results for the non-confining screening potentials like the Yukawa and Hulthén potentials [34–36], and its comparison against the physical heavy quarkonium spectrum is a crucial test for the Cornell potential. With this aim, we collected from the Review of Particle Properties [37], those states considered as "well established" and ordered them in ascending order of the mass values for bottomonium states in Table II and for charmonium states in Table III .

State	n	$^{2S+1}L_J$	$M_{exp}(GeV)$
$\Upsilon(4S)$	4	$^3S_1$	10.5794(1)
$\chi_{b2}(3P)$	4	$^3P_2$	10.5240(8)
$\chi_{b1}(3P)$	4	$^3P_1$	10.5134(7)
$\Upsilon(3S)$	3	$^3S_1$	10.3551(5)
$\chi_{b2}(2P)$	3	$^3P_2$	10.26865(72)
$h_b(2P)$	3	$^1P_1$	10.2598(12)
$\chi_{b1}(2P)$	3	$^3P_1$	10.25546(72)
$\chi_{b0}(2P)$	3	$^3P_0$	10.2325(9)
$\Upsilon_2(1D)$	3	$^3D_2$	10.1637(14)
$\Upsilon(2S)$	2	$^3S_1$	10.0234(5)
$\eta_b(2S)$	2	$^1S_0$	9.999(4)
$\chi_{b2}(1P)$	2	$^3P_2$	9.91221(57)
$h_b(1P)$	2	$^1P_1$	9.8993(8)
$\chi_{b1}(1P)$	2	$^3P_1$	9.89278(40)
$\chi_{b0}(1P)$	2	$^3P_0$	9.85944(73)
$\Upsilon(1S)$	1	$^3S_1$	9.46040(10)
$\eta_b(1S)$	1	$^1S_0$	9.3987(20)

TABLE II: Experimental results for the spectrum of the bottomonium [37]. All the states in this table are considered as well established by the Particle Data Group except for the $\eta_b(2S)$.

We can see in Table II that for $n = 2$, the $l = 0$ states, $\Upsilon(2S)$ and $\eta_b(2S)$, are heavier than the $l = 1$ states, $\chi_{b2}(1P), h_b(1P), \chi_{b1}(1P), \chi_{b0}(1P)$. Similar results hold for $n = 3$ where the $l = 0$ state, $\Upsilon(3S)$ (the $\eta_b(3S)$ state is missing), is heavier than the $l = 1$ states, $\chi_{b2}(2P), h_b(2P), \chi_{b1}(2P), \chi_{b0}(2P)$. In turn, these $l = 1$ states are heavier than the only $l = 2$ state so far discovered in this level, the $\Upsilon_2(1D)$ which is a 3^3D_2 state. The so far discovered bottomonium states in the $n = 4$ level follows the same pattern. *It is clear from the mass values in Table II that the physical spectrum of bottomonium follows the inverted spectrum pattern of the Bohr-like levels predicted by the complete analytical solution to the Cornell potential.*

The same pattern is clearly seen for the $n = 2$ level of charmonium. Indeed from the experimental mass values in Table III, we can see that in the $n = 2$ level, the $l = 0$ states $\psi(2s)$ and $\eta_c(2S)$ states are heavier than the $l=1$ states $\chi_{c2}(1P), h_c(1P), \chi_{c1}(1P), \chi_{c0}(1P)$. The identification of the $n^{2S+1}L_J$ charmonium states for $n \geq 3$ is unclear and from Table III we can see that there is an overpopulation of states and some of them cannot be conventional $\bar{q}q$ mesons.

An important physical quantity in heavy quarkonium physics is the size of a given quarkonium structure. This is important information for effective theories of QCD because it is precisely the inverse radius which fixes the scale of the soft modes. For the Coulomb interaction this information is usually obtained from the mean value of the inverse radius. With our complete analytical solution we can calculate the mean value of the inverse radius normalized to the Bohr radius for every n, l heavy quarkonium configuration as

$$a_Q r_{nl}^{-1}(\lambda) = \langle nl | \frac{a_Q}{r} | nl \rangle = a_Q \int_0^\infty dr r |R_{nl}(r, \lambda)|^2 \equiv f_{nl}^{(-1)}(\lambda). \tag{97}$$

We remark that the mean value of the inverse radius normalized by the Bohr radius is a function that depends only on the normalized string tension λ. In Fig. (4) we plot $f^{(-1)}(\lambda)$ for the lowest lying heavy quarkonium nl states, calculated with the [101/100] Padé approximant. We can see in this plot that $r_{nl}^{-1}(\lambda)$ goes from its l-independent Coulomb value $r_{nl}^{-1}(0) = 1/n^2 a_Q$, to a l-dependent value for the physical λ_Q, which increases with increasing λ.

State	n	$^{2S+1}L_J$	$M_{exp}(GeV)$
$\psi(4660)^*$	?	?	4.641(10)
$\psi(4415)$	?	$^3S_1$	4.415(5)
$\psi(4360)^*$	?	?	4.374(7)
$\chi_{c1}(4274)^*$	?	?	$4.286^{+0.008}_{-0.009}$
$\psi(4230)$	?	$^3S_1$	4.2221(23)
$\psi(4160)$	?	$^3S_1$	4.191(5)
$\chi_{c1}(4140)^*$	?	?	4.1465(30)
$\psi(4040)$	?	$^3S_1$	4.040(4)
$\chi_{c2}(3930)$	3	$^3P_2$	3.9225(10)
$\chi_{c0}(3915)^\dagger$	?	?	3.9221(18)
$\chi_{c1}(3872)^*$	?	?	3.87164(6)
$\psi(3842)$	?	$^3S_1$	3.84271(20)
$\psi(3823)$	?	$^3S_1$	3.82351(34)
$\psi(3770)$	?	$^3S_1$	3.7737(7)
$\psi(2S)$	2	$^3S_1$	3.686097(11)
$\eta_c(2S)$	2	$^1S_0$	3.6377(9)
$\chi_{c2}(1P)$	2	$^3P_2$	3.55617(7)
$h_c(1P)$	2	$^1P_1$	3.52537(14)
$\chi_{c1}(1P)$	2	$^3P_1$	3.51067(5)
$\chi_{c0}(1P)$	2	$^3P_0$	3.41471(30)
$J/\psi(1S)$	1	$^3S_1$	3.096900(6)
$\eta_c(1S)$	1	$^1S_0$	2.9841(4)

TABLE III: Charmonium spectrum collected from the Review of Particle Properties [37]. We list only those states considered as well established by the Particle Data Group. States marked with an asterisk are candidates to be exotic states. States marked with † are in doubt in their J^P assignement.
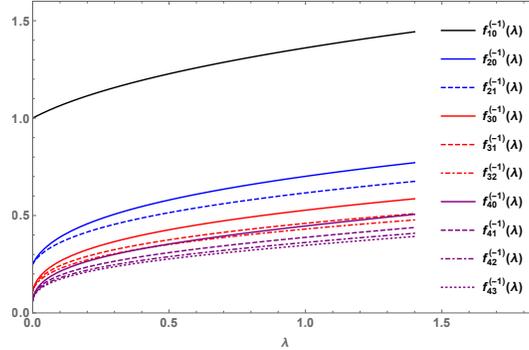
FIG. 4: Heavy quarkonium inverse mean radius in units of the Bohr radius, $\langle nl|(\frac{r}{a_Q})^{-1}|nl\rangle$, for the lowest lying states.

We conclude that heavy quarkonium states have smaller radius than the Coulomb states, being thus more compact systems.

A. Quantitative Bohr-like heavy quarkonium systems

The qualitative picture of quarkonium structure agrees with the measured heavy quarkonium spectrum and it would be interesting to do a quantitative analysis of the predictions in Eq. (94). A first estimate of the physical values of the parameters and involved quantities can be obtained considering that the Borh-like levels $\epsilon_{nl}(\lambda)$ correspond to the average values of the physical energies in each level. We expect relativistic corrections to be important for real heavy quarkonium systems thus the estimates in the remaining of this subsection must be considered only as a starting point

toward the description of real heavy quarkonium systems.

For a given n, the average values of the masses of the $l = 0, 1$ states are given by

$$\bar{M}_{n0}(\bar{\lambda}_Q) = \frac{1}{4} \left(M[n^1S_0] + 3M[n^3S_1] \right), \tag{98}$$

$$\bar{M}_{n1}(\bar{\lambda}_Q) = \frac{1}{12} \left(M[n^3P_0] + 3M[n^3P_1] + 5M[n^3P_2] + 3M[n^1P_1] \right), \tag{99}$$

where hereafter we use a bar for the physical quantities extracted from the physical average masses.

From the values for physical quarkonium in Tables II,III, we get the following average values for the $n = 1, 2$ bottomonium and charmonium levels

$$\bar{M}_{10}(\bar{\lambda}_b) = 9444.98 \pm 0.50 \ MeV, \qquad\qquad \bar{M}_{10}(\bar{\lambda}_c) = 3068.70 \pm 0.10 \ MeV, \tag{100}$$

$$\bar{M}_{20}(\bar{\lambda}_b) = 10017.30 \pm 1.07 \ MeV, \qquad\qquad \bar{M}_{20}(\bar{\lambda}_c) = 3674.00 \pm 0.22 \ MeV, \tag{101}$$

$$\bar{M}_{21}(\bar{\lambda}_b) = 9899.73 \pm 0.31 \ MeV, \qquad\qquad \bar{M}_{21}(\bar{\lambda}_c) = 3525.31 \pm 0.05 \ MeV. \tag{102}$$

It is convenient for the purposes of this subsection to rewrite Eq. (94) as

$$\bar{M}_{nl}(\bar{\lambda}_Q) = \mu_Q(\bar{m}_Q) + \mu_B(\bar{m}_Q)\epsilon_{nl}(\bar{\lambda}_Q). \tag{103}$$

The Bohr level values of $\bar{\lambda}_Q$, can be obtained from these relations for $n = 1, 2$ as the solution to

$$\frac{\epsilon_{20}(\bar{\lambda}_Q) - \epsilon_{10}(\bar{\lambda}_Q)}{\epsilon_{20}(\bar{\lambda}_Q) - \epsilon_{21}(\bar{\lambda}_Q)} = \frac{\bar{M}_{20}(\bar{\lambda}_Q) - \bar{M}_{10}(\bar{\lambda}_Q)}{\bar{M}_{20}(\bar{\lambda}_Q) - \bar{M}_{21}(\bar{\lambda}_Q)}. \tag{104}$$

The experimental values for the ratio on the right hand side are obtained from the average values in Eqs. (100,101,102) as

$$\frac{\bar{M}_{20}(\bar{\lambda}_b) - \bar{M}_{10}(\bar{\lambda}_b)}{\bar{M}_{20}(\bar{\lambda}_b) - \bar{M}_{21}(\bar{\lambda}_b)} = 4.868 \pm 0.035, \qquad \frac{\bar{M}_{20}(\bar{\lambda}_c) - \bar{M}_{10}(\bar{\lambda}_c)}{\bar{M}_{20}(\bar{\lambda}_c) - \bar{M}_{21}(\bar{\lambda}_c)} = 4.071 \pm 0.005. \tag{105}$$

Solving equation (104) for bottomonium and charmonium we get the following Bohr values of the normalized string tension at the heavy quarkonium scales

$$\bar{\lambda}_b = 0.884 \pm 0.023, \qquad \bar{\lambda}_c = 1.694 \pm 0.009. \tag{106}$$

The values of the energy levels at the Bohr values of the normalized string tension for heavy quarkonium are

$$\epsilon_{10}(\bar{\lambda}_b) = 0.073 \pm 0.024, \qquad\qquad \epsilon_{10}(\bar{\lambda}_c) = 0.875 \pm 0.008, \tag{107}$$

$$\epsilon_{20}(\bar{\lambda}_b) = 2.527 \pm 0.056, \qquad\qquad \epsilon_{20}(\bar{\lambda}_c) = 4.299 \pm 0.018, \tag{108}$$

$$\epsilon_{21}(\bar{\lambda}_b) = 2.014 \pm 0.045, \qquad\qquad \epsilon_{21}(\bar{\lambda}_c) = 3.458 \pm 0.015. \tag{109}$$

The values of the scales $\mu_Q(m_Q)$ and $\mu_B(m_Q)$ are obtained as

$$\mu_B(\bar{m}_Q) = \frac{\bar{M}_{20}(\bar{\lambda}_Q) - \bar{M}_{10}(\bar{\lambda}_Q)}{\epsilon_{20}(\bar{\lambda}_Q) - \epsilon_{10}(\bar{\lambda}_Q)}, \tag{110}$$

$$\mu_Q(\bar{m}_Q) = \frac{\epsilon_{20}(\bar{\lambda}_Q)\bar{M}_{10}(\bar{\lambda}_Q) - \epsilon_{10}(\bar{\lambda}_Q)\bar{M}_{20}(\bar{\lambda}_Q)}{\epsilon_{20}(\bar{\lambda}_Q) - \epsilon_{10}(\bar{\lambda}_Q)}. \tag{111}$$

The values obtained for the energy scales at the Bohr values of the normalized string tension are

$$\mu_B(\bar{m}_b) = 233.25 \pm 5.80 \ MeV, \qquad\qquad \mu_B(\bar{m}_c) = 176.8 \pm 1.0 \ MeV, \tag{112}$$

$$\mu_Q(\bar{m}_b) = 9427.92 \pm 5.91 \ MeV, \qquad\qquad \mu_Q(\bar{m}_c) = 2914.0 \pm 4.2 \ MeV. \tag{113}$$

These values for the physical scales yields the following values for the strong coupling constant and heavy quark masses

$$\bar{m}_b = 4713.96 \pm 2.95.5 \ MeV, \qquad\qquad \alpha_s(\bar{m}_b) = 0.3337 \pm 0.0041, \tag{114}$$

$$\bar{m}_c = 1457.0 \pm 2.1 \ MeV, \qquad\qquad \alpha_s(\bar{m}_c) = 0.5225 \pm 0.0016. \tag{115}$$

We must warn that these values are obtained in an $\mathcal{O}(v^2)$ calculation and should be considered only as a first approximation to the real values. There is also a lot of sensitivity to the used input, e.g. using instead the values of the masses of the $n = 1, 2, 3$ n^3S_1 bottomonium states we get $\lambda_b \approx 0.4$ and similar values for $\alpha_s(m_b)$ and $\mu_Q(m_b), \mu_B(m_b)$.

Once fixed the Bohr values of $\bar{\lambda}_Q$ and of the energy scales we obtain the following values for the energy of the $n = 3, 4$ excited states

$$\epsilon_{30}(\bar{\lambda}_b) = 4.121 \pm 0.080, \quad \epsilon_{30}(\bar{\lambda}_c) = 6.666 \pm 0.026, \tag{116}$$

$$\epsilon_{31}(\bar{\lambda}_b) = 3.663 \pm 0.071, \quad \epsilon_{31}(\bar{\lambda}_c) = 5.919 \pm 0.023, \tag{117}$$

$$\epsilon_{32}(\bar{\lambda}_b) = 3.128 \pm 0.062, \quad \epsilon_{32}(\bar{\lambda}_c) = 5.076 \pm 0.020, \tag{118}$$

$$\epsilon_{40}(\bar{\lambda}_b) = 5.448 \pm 0.103, \quad \epsilon_{40}(\bar{\lambda}_c) = 8.762 \pm 0.035, \tag{119}$$

$$\epsilon_{41}(\bar{\lambda}_b) = 5.024 \pm 0.095, \quad \epsilon_{41}(\bar{\lambda}_c) = 8.067 \pm 0.032, \tag{120}$$

$$\epsilon_{42}(\bar{\lambda}_b) = 4.537 \pm 0.086, \quad \epsilon_{42}(\bar{\lambda}_c) = 7.292 \pm 0.029, \tag{121}$$

$$\epsilon_{43}(\bar{\lambda}_b) = 4.028 \pm 0.076, \quad \epsilon_{43}(\bar{\lambda}_c) = 6.488 \pm 0.026, \tag{122}$$

and from Eq. (103) the following predictions of the Cornell potential for the average masses of the $n = 3, 4$ excited states are obtained

$$\bar{M}_{30}(\bar{\lambda}_b) = 10389.10 \pm 30.9 \ MeV, \qquad \bar{M}_{30}(\bar{\lambda}_c) = 4092.46 \pm 9.41 \ MeV, \tag{123}$$

$$\bar{M}_{31}(\bar{\lambda}_b) = 10282.2 \pm 27.6 \ MeV, \qquad \bar{M}_{31}(\bar{\lambda}_c) = 3960.52 \pm 8.58 \ MeV, \tag{124}$$

$$\bar{M}_{32}(\bar{\lambda}_b) = 10157.4 \pm 23.9 \ MeV, \qquad \bar{M}_{32}(\bar{\lambda}_c) = 3811.48 \pm 7.69 \ MeV, \tag{125}$$

$$\bar{M}_{40}(\bar{\lambda}_b) = 10698.7 \pm 40.17 \ MeV, \qquad \bar{M}_{40}(\bar{\lambda}_c) = 4463.19 \pm 11.87 \ MeV, \tag{126}$$

$$\bar{M}_{41}(\bar{\lambda}_b) = 19599.8 \pm 37.1 \ MeV, \qquad \bar{M}_{41}(\bar{\lambda}_c) = 4340.29 \pm 11.04 \ MeV, \tag{127}$$

$$\bar{M}_{42}(\bar{\lambda}_b) = 10486.2 \pm 33.6 \ MeV, \qquad \bar{M}_{42}(\bar{\lambda}_c) = 4203.22 \pm 10.15 \ MeV, \tag{128}$$

$$\bar{M}_{43}(\bar{\lambda}_b) = 10367.4 \pm 30.0 \ MeV, \qquad \bar{M}_{43}(\bar{\lambda}_c) = 4061 \pm 9.25 \ MeV. \tag{129}$$

Comparing with the average values extracted from Table II in the bottomonium sector we can see that these values are slightly above the existing data. We conclude that although the non-relativistic description of heavy quarkonium structure given by the Cornell potential captures all the qualitative features of these systems, the description of real heavy quarkonium requires to consider relativistic corrections. In this concern, aiming to get insight into the importance of relativistic corrections for the different heavy quarkonium configurations, it is interesting to calculate the mean value of v^2, given by

$$\langle nl|v^2|nl \rangle = \frac{4}{m_Q} \langle nl|H_0 + \frac{4\alpha_s}{3r} - \sigma r|nl \rangle = \alpha_s^2 C_{nl}(\lambda), \tag{130}$$

with

$$C_{nl}(\lambda) = \frac{16}{9} \left(\epsilon_{nl}(\lambda) + 2f_{nl}^{(-1)}(\lambda) - \lambda f_{nl}^{(1)}(\lambda) \right), \tag{131}$$

where

$$f_{nl}^{(k)}(\lambda) \equiv \langle nl| \left(\frac{r}{a_Q} \right)^k |nl \rangle = a_Q^{-k} \int_0^{\infty} dr r^{2+k} |R_{nl}(r)|^2. \tag{132}$$

are dimensionless functions depending only on λ.

Using the virial theorem it can be shown that for the Cornell potential

$$\epsilon_{nl}(\lambda) = -f_{nl}^{(-1)}(\lambda) + \frac{3}{2} \lambda f_{nl}^{(1)}(\lambda), \tag{133}$$

and the proportionality constant can also be written as

$$C_{nl}(\lambda) = \frac{8}{9} \left(2f_{nl}^{(-1)}(\lambda) + \lambda f_{nl}^{(1)}(\lambda) \right). \tag{134}$$

Equations (130,134) show that the average value of v^2 is indeed proportional of α_s^2 as expected from the NRQCD counting rules. However, the proportionality constant depends in a complicated manner on the string tension. The
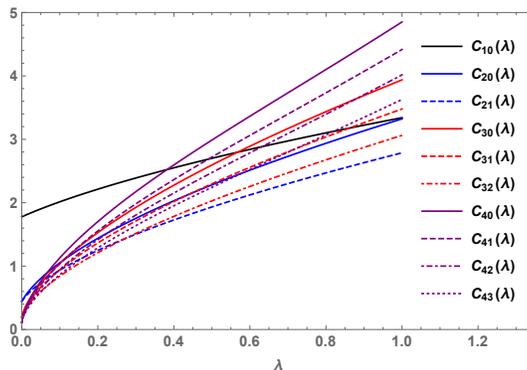
FIG. 5: Proportionality constant $C_{nl}(\lambda)$ between $\langle nl|v^2|nl\rangle$ and α_s^2 as a function of λ for the lowest lying states.

detail of this dependence can be obtained from our complete solution to the Cornell potential and it is shown in Fig. (5) where we plot the proportionality constant C_{nl} as a function of λ for the lowest lying $n = 1, 2, 3, 4$ states, calculated with the $[101/100]$ Padé approximant. We can see in this plot that the proportionality constant changes its beahaviour from its Coulombian value $C_{nl}(0) = \frac{16}{9n^2}$ decreasing with n and l-independent, to a value around 2 which is l-dependent, for $\lambda \approx 0.4$. The general lesson from this plot is that relativistic corrections will be more important than expected for heavy quarkonium systems, although a precise quantification of this effect must await for a more precise extraction of the value of λ_Q from data. We devote the next section to the calculation of the leading relativistic corrections which in addition to modify the predictions for the Bohr levels break the m-degeneracy in $\epsilon_{nl}(\lambda)$ through the spin-dependent interactions. In preparation, we notice that there is an obvious mass hierarchy in the experimental fine splittings of heavy quarkonium which can be seen in Tables II, III. Indeed, from the measured values of the masses of the $n = 1$ and $n = 2$ levels of heavy quarkonium, systematically for the s-waves, the n^3S_1 state is heavier that the n^1S_0 state. Also, for the $n = 2$ and $n = 3$ (in the bottomonium case) p-wave states, the masses are such that systematically $M_{\chi_{b2}(nP)} > M_{h_b(nP)} > M_{\chi_{b1}(nP)} > M_{\chi_{b0}(nP)}$.

IV. REAL HEAVY QUARKONIUM: LEADING RELATIVISTIC CORRECTIONS

Relativistic corrections are expected from Eq. (130) to be of order α_s^4 and to yield a closer approach to real heavy quarkonium systems. The derivation of the leading relativistic corrections has been done using diverse methods [5–11, 18, 38] and the corresponding operators can be classified into spin-independent and spin-dependent interactions. The leading spin-independent corrections include conventional corrections to the kinetic energy and velocity-dependent terms [10, 11], which shifts the Bohr-like energy levels $\epsilon_{nl}(\lambda)$ but do not remove the m-degeneracy of the l orbitals for a fixed n. It is not the aim of this work to do a complete phenomenological analysis of the relativistic corrections and we will focus only on the fine splittings in heavy quarkonium produced by the spin-dependent interactions. However, there are interesting conclusions arising from this analysis concerning the $1/m_Q$ expansion and we will consider explicitly the corrections to the kinetic energy in the spin-independent sector to illustrate the point. These corrections are induced by

$$H_K = -\frac{p^4}{4m_Q^3} = -\frac{1}{4m_Q}\left(H_0 + \frac{4}{3}\frac{\alpha_s}{r} - \frac{8}{27}m_Q^2\alpha_s^3\lambda r\right)^2. \tag{135}$$

The corrections to E_{nl} due to this term, as calculated in perturbation theory are given by

$$\Delta E_{nl}^{si} = -\frac{4}{81}m_Q\alpha_s^4\left(\epsilon_{nl}^2(\lambda) + 4f_{nl}^{(-2)}(\lambda) + \lambda^2 f_{nl}^{(2)}(\lambda) + 4\epsilon_{nl}(\lambda)f_{nl}^{(-1)}(\lambda) - 2\lambda\epsilon_{nl}(\lambda)f_{nl}^{(1)}(\lambda) - 4\lambda\right). \tag{136}$$

A. Spin-dependent interactions

The proper description of the physical spectrum of heavy quarkonium requires to consider the spin-dependent interactions responsible for the splitting of the Bohr energy levels $\epsilon_{nl}(\lambda)$. These interactions arise from the leading

relativistic corrections and for the Cornell potential are given by

$$H_{SD} = \frac{8\alpha_s}{9m_Q^2} \boldsymbol{S}_1 \cdot \boldsymbol{S}_2 \frac{\delta(r)}{r^2} + \frac{2\alpha_s}{m_Q^2} \frac{\boldsymbol{L} \cdot \boldsymbol{S}}{r^3} + \frac{\alpha_s}{3m_Q^2} \frac{S_{12}}{r^3} - \frac{\sigma}{2m_Q^2} \frac{\boldsymbol{L} \cdot \boldsymbol{S}}{r}, \tag{137}$$

where

$$S_{12} = 4[3(\boldsymbol{S}_1 \cdot \hat{\boldsymbol{r}})(\boldsymbol{S}_2 \cdot \hat{\boldsymbol{r}}) - \boldsymbol{S}_1 \cdot \boldsymbol{S}_2]. \tag{138}$$

The leading relativistic corrections have a $1/m_Q^2$ suppression and are expected to be small. The first term in Eq. (137) is the analogous of the hyperfine splitting in atomic physics where it is suppressed due to the small electron to proton mass ratio. Here, this term is of the same order as the remaining fine structure terms and we will denote all terms in Eq. (137) as fine structure interactions. We can treat these interactions perturbatively due to their formal $1/m_Q^2$ suppression. To leading order we need to calculate the spin-dependent matrix elements

$$\langle \bar{Q}Q[n^{2S+1}L_J]|O_i|\bar{Q}Q[n^{2S+1}L_J]\rangle, \tag{139}$$

for $O_1 = \boldsymbol{S}_1 \cdot \boldsymbol{S}_2 \frac{\delta(r)}{r^2}$, $O_2 = \frac{\boldsymbol{L} \cdot \boldsymbol{S}}{r^3}$, $O_3 = \frac{S_{12}}{r^3}$ and $O_4 = \frac{\boldsymbol{L} \cdot \boldsymbol{S}}{r}$. The angular momentum part yields the well defined n-independent factors

$$\langle \boldsymbol{S}_1 \cdot \boldsymbol{S}_2 \rangle = \frac{1}{2}\left[s(s+1) - \frac{3}{2}\right], \tag{140}$$

$$\langle \boldsymbol{L} \cdot \boldsymbol{S} \rangle = \frac{1}{2}[j(j+1) - l(l+1) - s(s+1)], \tag{141}$$

$$\langle S_{12} \rangle = \frac{2[2l(l+1)s(s+1) - 3\langle \boldsymbol{L} \cdot \boldsymbol{S} \rangle - 6\langle \boldsymbol{L} \cdot \boldsymbol{S} \rangle^2]}{(2l-1)(2l+3)}. \tag{142}$$

The explicit spin factors for the lowest lying angular momentum configurations are given in Table IV.

Operator	$^1S_0$	$^3S_1$	$^1P_1$	$^3P_0$	$^3P_1$	$^3P_2$	$^1D_2$	$^3D_1$	$^3D_2$	$^3D_3$
$\langle \boldsymbol{S}_1 \cdot \boldsymbol{S}_2 \rangle$	$-\frac{3}{4}$	$\frac{1}{4}$	$-\frac{3}{4}$	$\frac{1}{4}$	$\frac{1}{4}$	$\frac{1}{4}$	$-\frac{3}{4}$	$\frac{1}{4}$	$\frac{1}{4}$	$\frac{1}{4}$
$\langle \boldsymbol{L} \cdot \boldsymbol{S} \rangle$	0	0	0	-2	-1	1	0	-3	-1	2
$\langle S_{12} \rangle$	0	0	0	-4	2	$-\frac{2}{5}$	0	-2	2	$-\frac{4}{7}$

TABLE IV: Spin factors for the lowest lying angular momentum configurations.

The corrections to E_{nl} due to the spin-dependent term to the mass of heavy quarkonium, as calculated in perturbation theory, are given by

$$\Delta E_{nl}^{sd}(\lambda) = \frac{8\alpha_s}{9m_Q^2}\langle \boldsymbol{S}_1 \cdot \boldsymbol{S}_2 \rangle \left\langle \frac{\delta(r)}{r^2} \right\rangle_{nl}$$
$$+ \left(\frac{2\alpha_s}{m_Q^2}\left\langle \frac{1}{r^3} \right\rangle_{nl} - \frac{\sigma}{2m_Q^2}\left\langle \frac{1}{r} \right\rangle_{nl}\right)\langle \boldsymbol{L} \cdot \boldsymbol{S} \rangle + \frac{\alpha_s}{3m_Q^2}\langle S_{12} \rangle \left\langle \frac{1}{r^3} \right\rangle_{nl}. \tag{143}$$

This result can be written as

$$\Delta E_{nl}^{sd}(\lambda) = \frac{16}{243}m_Q\alpha_s^4\left[f_{nl}^{ss}(\lambda)4\langle \boldsymbol{S}_1 \cdot \boldsymbol{S}_2 \rangle + \left(9f_{nl}^{(-3)}(\lambda) - \frac{3}{2}\lambda f_{nl}^{(-1)}(\lambda)\right)\langle \boldsymbol{L} \cdot \boldsymbol{S} \rangle + \frac{3}{2}f_{nl}^{(-3)}(\lambda)\langle S_{12} \rangle\right], \tag{144}$$

where

$$f_{nl}^{ss}(\lambda) = a_Q^3 \int_0^\infty \delta(r)|R_{nl}(r,\lambda)|^2 = a_Q^3|R_{nl}(0,\lambda)|^2 \tag{145}$$

and $f^{(k)}(\lambda)$ are given in Eq. (132).

B. Heavy quarkonium spectrum to order α_s^4

Considering both spin-independent and spin-dependent interactions, the mass of heavy quarkonium in a $n^{2S+1}L_J$ configuration to order α_s^4 is given by

$$M[n^{2S+1}L_J] = 2m_Q + \frac{4}{9}m_Q\alpha_s^2\epsilon_{nl}(\lambda) - \frac{64}{243}m_Q\alpha_s^4\Delta_{nl}^{SI}(\lambda)$$
$$+ \frac{64}{243}m_Q\alpha_s^4\left[f_{nl}^{ss}(\lambda)\langle \boldsymbol{S}_1 \cdot \boldsymbol{S}_2\rangle + \left(\frac{9}{4}f_{nl}^{(-3)}(\lambda) - \frac{3}{8}\lambda f_{nl}^{(-1)}(\lambda)\right)\langle \boldsymbol{L} \cdot \boldsymbol{S}\rangle + \frac{3}{8}f_{nl}^{(-3)}(\lambda)\langle S_{12}\rangle\right]. \tag{146}$$

with

$$\Delta_{nl}^{SI}(\lambda) = \frac{3}{16}\epsilon_{nl}^2(\lambda) + \frac{3}{4}f_{nl}^{(-2)}(\lambda) + \frac{3}{16}\lambda^2 f_{nl}^{(2)}(\lambda) + \frac{3}{8}\epsilon_{nl}(\lambda)\left(2f_{nl}^{(-1)}(\lambda) - \lambda f_{nl}^{(1)}(\lambda)\right) - \frac{3}{4}\lambda. \tag{147}$$

This is the second main result of this paper and there are several worth remarks on Eq. (146). Firstly, notice that the formal $1/m_Q^2$ suppression of the spin-dependent interactions in Eq. (137) is cancelled by the m_Q dependence of the involved matrix elements. This result arises from our choice of the Bohr radius as the reference dimension scale, thus the average value *e.g.* of $\langle 1/r^3\rangle_{nl}$ must be proportional to $1/a_Q^3 \approx m_Q^3\alpha_s^3$. This is also valid for the velocity-dependent terms in the spin-dependent sector not shown here.

Secondly, with this result, we get actually a consistent expansion in powers of α_s^2 for the masses of heavy quarkonium. Al leading order we simply get the perturbative physics scale $\mu_Q = 2m_Q$. At order α_s^2, the coefficient is given by $\frac{4}{9}m_Q\epsilon_{nl}(\lambda)$ and involves non-perturbative QCD effects mimicked by the string tension λ. This coefficient is actually different for the different quarkonium configurations. The different coefficients are calculated exactly here and involve the analytic solution for the normalized energies of the Cornell potential, $\epsilon_{nl}(\lambda)$. For the quarkonium spectrum, the non-perturbative effects manifest at order α_s^2 in the λ dependence of $\epsilon_{nl}(\lambda)$, which is responsible for the breaking of the l-degeneracy of the n-levels of the Coulomb-like interaction. The order α_s^4 corrections include spin-independent and spin-dependent interactions and their non-perturbative effects are calculated using Rayleigh-Schrödinger perturbation theory. Our approximate calculation of these effects shows that the size of non perturbative effects at this order are modulated by the mean values of the space part of the corresponding operators which also involve the probabilities of the Cornell potential, $|R_{nl}(r,\lambda)|^2$.

These results show that, for the heavy quarkonium spectrum, the suppression of higher order terms in the non-relativistic expansion (including non-perturbative effects) depends only on the expansion in $\alpha_s^2(m_Q)$ and the whole expansion makes sense as long as $\alpha_s(m_Q)$ is still small, which we expect to be satisfied for heavy quarkonium. Notice that Eq. (146) is consistent with the power counting rules of NRQCD, where we have a perturbative scale m_Q and non-perturbative effects are suppressed by powers of $v^2 \approx \alpha_s^2(m_Q)$. In this concern, we remark that in Eq. (146) a new scale appear, given by

$$\mu_f(m_Q) = \frac{64}{243}m_Q\alpha_s^4. \tag{148}$$

which is the natural scale of the fine splittings of the heavy quarkonium spectrum.

The mass hierarchies in the fine splittings of the measured heavy quarkonium spectrum noticed at the end of the previous section can be understood from Eq. (146) and the values of average spin-dependent operators in Table IV. Indeed, notice that Eq. (146) can be written as

$$M[n^{2S+1}L_J] = M_{nl}^{SI}(\lambda) + M^{SD}[n^{2S+1}L_J](\lambda) \tag{149}$$

where the spin-independent part, $M_{nl}^{SI}(\lambda)$, contain terms of order α_s^2 and α_s^4 which, for a given n, still preserve the m-degeneracy of the l-levels. This degeneracy is broken by the spin-dependent contribution $M^{SD}[n^{2S+1}L_J](\lambda)$ which only contains terms of order α_s^4 producing the fine splittings of heavy quarkonium.

From the mean values of the spin operators in Table IV, we can see that the spin-dependent contribution to the masses of the $l = 0$ states in a given level n, get contributions of the spin-spin interactions only and we obtain

$$M[n^3S_1] - M[n^1S_0] = \mu_f \, f_{nl}^{ss}(\lambda) > 0, \tag{150}$$

thus the n^3S_1 states are heavier than the n^1S_0 states. This pattern is exhibited by the $n = 1, 2$ levels of heavy quarkonium as discussed at the end of the previous section and we predict this behavior to be valid for every level n in both heavy quarkonium sectors.
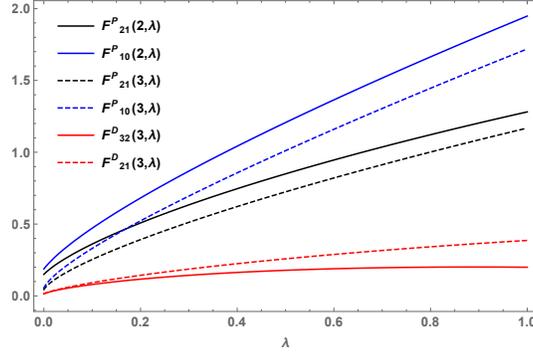
FIG. 6: Combinations $F_{21}^P(2,\lambda), F_{10}^P(2,\lambda), F_{21}^P(3,\lambda), F_{10}^P(3,\lambda), F_{32}^D(2,\lambda), F_{21}^D(3,\lambda)$ appearing in Eqs. (151, 152,153,154) for $n = 2,3$, as functions of λ.

The ordering of the ^3P_J states in a given level n can also be obtained from Eq. (146). Indeed, a straightforward calculation using the spin factors Table IV yields

$$M[n^3P_2] - M[n^3P_1] = \mu_f \left(\frac{18}{5} f_{n1}^{(-3)}(\lambda) - \frac{3}{4}\lambda f_{n1}^{(-1)}(\lambda) \right) \equiv \mu_f F_{21}^P(n,\lambda), \tag{151}$$

$$M[n^3P_1] - M[n^3P_0] = \mu_f \left(\frac{9}{2} f_{n1}^{(-3)}(\lambda) - \frac{3}{8}\lambda f_{n1}^{(-1)}(\lambda) \right) \equiv \mu_f F_{10}^P(n,\lambda). \tag{152}$$

As for the D-waves in the n level, the mass splittings are given by

$$M[n^3D_3] - M[n^1D_2] = \mu_f \left(\frac{81}{14} f_{n2}^{(-3)}(\lambda) - \frac{9}{8}\lambda f_{n2}^{(-1)}(\lambda) \right) \equiv \mu_f F_{32}^D(n,\lambda), \tag{153}$$

$$M[n^3D_2] - M[n^3D_1] = \mu_f \left(6 f_{n2}^{(-3)}(\lambda) - \frac{3}{4}\lambda f_{n2}^{(-1)}(\lambda) \right) \equiv \mu_f F_{21}^D(n,\lambda). \tag{154}$$

In Fig. (6) we plot the functions $F_{21}^P(n,\lambda), F_{10}^P(n,\lambda), F_{32}^D(n,\lambda), F_{21}^D(n,\lambda)$ for $n = 2,3$, calculated with the [101/100] Padé approximant, where we can see that these functions are positive. This results yields the ordering

$$M[n^3P_2] > M[n^3P_1] > M[n^3P_0] \tag{155}$$

for $n = 2,3$ states and

$$M[n^3D_3] > M[n^3D_2] > M[n^3D_1] \tag{156}$$

for $n = 3$. This ordering is clearly seen in the physical spectrum of bottomonium for the $2^3P_J, 3^3P_J$ and 3^3D_J states. In the case of charmonium, the measured 2^3P_J states also exhibit this ordering. We predict that the $n = 3$ P- and D-waves charmonium states satisfy also this ordering. Notice that even at the qualitative level discussed in this section, both the inverted spectrum and the order α_s^4 corrections obtained here yields a consistent picture of the heavy quarkonium spectrum.

V.   ASESSING NON-PERTURBATIVE EFFECTS AND PREDICTIONS FOR THE MISSING HEAVY QUARKONIUM STATES

It is not the aim of the present work to give a detailed numerical analysis of the predictions of the complete analytical solution of the Cornell potential and the leading relativistic corrections obtained here for the quarkonium spectrum, but it would be interesting to have an idea of the numerical value of the physical normalized string tension λ_Q which in the Cornell potential mimmicks non-perturbative QCD effects. In this section we will obtain it confidently from the fine splittings. It will allow us to make well defined predictions on the mass values of some missing states and on the range of mass values where other missing heavy quarkonium states must lie, which is relevant for the experimental searches of these states. In particular, in the charmonium spectrum we have an overpopulation of states and, in addition to the search for the missing $\bar{c}c$ states, the identification of the $\bar{c}c$ states among the so far discovered mesons

is very important to identify the non-conventional mesons and to focus the effort in the study of their properties aiming to elucidate their nature.

In this concern, we can see from Eq. (150) that the fine splittings in the S-wave sectors are dictated by the fine energy scale μ_f and the value of $f_{nl}^{ss}(\lambda)$ at the physical value λ_Q. The value of λ_Q can be estimated considering the ratio

$$\frac{M[2^3S_1] - M[2^1S_0]}{M[1^3S_1] - M[1^1S_0]} = \frac{f_{20}^{ss}(\lambda_Q)}{f_{10}^{ss}(\lambda_Q)}. \tag{157}$$

For a confident extraction from data of the physical value λ_Q, it is important to remark that the normalized wave function at the origin, $f_{n0}^{ss}(\lambda_Q)$, actually receive considerable radiative corrections as noticed in [6]. These corrections cancel in the ratio of the normalized wavefunctions in Eq. (157) and a reliable estimate of λ_Q for heavy quarkonium can be obtained from this equation, which is independent of the α_s and m_Q factors. The ratio on the right hand side can be obtained from the complete analytical solution to the Cornell potential and depends only on λ. The experimental value of the left hand side of this equation can be extracted from Tables II and III and we get

$$\frac{M[\Upsilon(2S)] - M[\eta_b(2S)]}{M[\Upsilon(1S)] - M[\eta_b(1S)]} = 0.395 \pm 0.017, \tag{158}$$

$$\frac{M[\psi(2S)] - M[\eta_c(2S)]}{M[J/\psi(1S)] - M[\eta_c(1S)]} = 0.429 \pm 0.008. \tag{159}$$

The dimensionless functions $f_{nl}^{ss}(\lambda)$ are related to $R_{nl}^2(0,\lambda)$ by Eq. (145). We reconstructed $R_{10}^2(0,\lambda)$ and $R_{20}^2(0,\lambda)$ using the [151/150] and [150/150] Padé approximants. With these reconstructed functions, solving Eq. (157) we get the following values for the physical normalized string tension at the bottomonium and charmonium mass scales

$$\lambda_b = 0.361 \pm 0.054, \tag{160}$$

$$\lambda_c = 0.482 \pm 0.033. \tag{161}$$

Notice that these values are considerably lower than those extracted from the Bohr-like levels in Eq. (106). Also, for excited states, these values are very large compared with the critical values listed in Table I.

Once fixed the physical values of λ_Q, from our complete analytical solution we can calculate the numerical factors $\epsilon_{nl}(\lambda_Q)$ and $f_{nl}^{ss}(\lambda_Q)$ which are collected in Table V for values up to $n = 4$. To this end we use the $\epsilon_{nl}(\lambda)$ and $f_{nl}^{ss}(\lambda)$ functions reconstructed with the [151/150] and [150/150] Padé approximants. The actual value of the corresponding functions lie between these approximants and we estimate the uncertainty in the reconstruction as the ratio of the difference and the sum of these functions. We list the theoretical uncertainties in the calculation of the physical quantities in the last column of Table V.

A. Bottomonium

The fine structure scale for bottomonium can be obtained from Eq. (150) which yields

$$\mu_f(m_b) = \frac{M[\Upsilon(1S) - M[\eta_b(1S)]}{f_{10}^{ss}(\lambda_b)} = 10.86 \pm 0.54 \ MeV. \tag{162}$$

As a cross check, we obtain the same value if we use instead data on the $n = 2$, S-wave states.

We can see in Table II that states in the $n = 1, 2$ levels are complete and follow the inverted spectrum pattern predicted by the Cornell potential and the P-waves ordering obtained from the leading relativistic corrections. For $n \geq 3$ the states $\eta_b(nS)$ are missing. The value of the masses of these states can be obtained from Eq. (150) as

$$M[\eta_b(nS)] = M[\Upsilon(nS)] - \mu_f(m_b)f_{n0}^{ss}(\lambda_b). \tag{163}$$

Using the values for $f_{30}^{ss}(\lambda_b)$ and $f_{40}^{ss}(\lambda_b)$ quoted in Table V, and the experimental values for the masses of the $\Upsilon(3S)$ and $\Upsilon(4S)$ in Table II we predict the masses of the missing $\eta_b(3S)$ and $\eta_b(4S)$ as

$$M[\eta_b(3S)] = 10337 \pm 2 \ MeV, \tag{164}$$

$$M[\eta_b(4S)] = 10564 \pm 2 \ MeV. \tag{165}$$

As to the D-wave states in the $n = 3$ level with configurations 3^3D_3, 3^1D_2, 3^3D_2 and 3^1D_1, only the 3^3D_2 (the $\Upsilon_2(1D)$) has been discovered with a mass $M[\Upsilon_2(1D)] = 10163.7 \ MeV$. The ordering of D-wave states in Eq. (156)

Observable	Value	Uncertainty
λ_b	0.361 ± 0.054	
λ_c	0.482 ± 0.033	
$\epsilon_{10}(\lambda_b)$	-0.518 ± 0.06	1.0×10^{-16}
$\epsilon_{20}(\lambda_b)$	1.124 ± 0.165	2.1×10^{-13}
$\epsilon_{30}(\lambda_b)$	2.070 ± 0.245	2.1×10^{-7}
$\epsilon_{40}(\lambda_b)$	2.828 ± 0.314	6.8×10^{-5}
$\epsilon_{10}(\lambda_c)$	-0.374 ± 0.039	7.4×10^{-17}
$\epsilon_{20}(\lambda_c)$	1.480 ± 0.094	1.1×10^{-11}
$\epsilon_{30}(\lambda_c)$	2.596 ± 0.138	1.8×10^{-6}
$\epsilon_{40}(\lambda_c)$	3.500 ± 0.176	2.7×10^{-4}
$f_{10}^{ss}(\lambda_b)$	5.681 ± 0.212	7.8×10^{-17}
$f_{20}^{ss}(\lambda_b)$	2.246 ± 0.182	2.9×10^{-13}
$f_{30}^{ss}(\lambda_b)$	1.681 ± 0.155	2.8×10^{-7}
$f_{40}^{ss}(\lambda_b)$	1.440 ± 0.141	8.0×10^{-5}
$f_{10}^{ss}(\lambda_c)$	6.140 ± 0.121	$< 1 \times 10^{-17}$
$f_{20}^{ss}(\lambda_c)$	2.634 ± 0.101	1.5×10^{-11}
$f_{30}^{ss}(\lambda_c)$	2.014 ± 0.087	2.2×10^{-6}
$f_{40}^{ss}(\lambda_c)$	1.743 ± 0.080	3.0×10^{-4}

TABLE V: Numerical values of observables relevant for the calculation of the spectrum of the S-wave states of heavy quarkonium, obtained from the eigenvalues and eigenstates of the Cornell potential, reconstructed with the $[151/150]$ Padé approximant from the corresponding series calculated to order λ^{301}.

and the inverted spectrum requires the masses of the 3^3D_3, 3^1D_2 states to be in range $[10163, 10232]\ MeV$. Similarly, the mass of the 3^1D_1 state is predicted to be in the $[10023, 10163]\ MeV$ range.

Concerning the states in the $n = 4$ level of bottomonium, we have the following missing P, D and F-wave states: $4^1P_1, 4^3P_0, 4^3D_3, 4^1D_2, 4^3D_2, 4^3D_1, 4^3F_4, 4^1F_3, 4^3F_3, 4^3F_2$. Our complete analytical solution predicts all these states to be below the $\chi_{b2}(3P)$ state, and above the $\Upsilon(3S)$ state, i.e. in the energy range $[10355, 10524]MeV$, with P states being heavier than the D states which in turn are more massive than the F states. In particular, the F states must be around the mass of the $\Upsilon(3S)$ state because it is precisely with these levels where the crossing phenomena starts.

B.   Charmonium

The values of the masses for charmonium states listed in Table III shows that states in the $n = 1, 2$ levels are complete and follow the inverted spectrum pattern predicted by the Cornell potential. Also, the ordering of the P-waves follows the pattern predicted by the leading relativistic corrections. We can extract the value of the fine structure scale for charmonium from Eq. (150) and data on the $n = 1$, S-wave states which yields

$$\mu_f(m_c) = \frac{M[J/\psi(1S)] - M[\eta_c(1S)]}{f_{10}^{ss}(\lambda_c)} = 18.37 \pm 0.36\ MeV. \tag{166}$$

We cross checked this result using instead data of the $n = 2$, S-wave charmonium states obtaining the same value.

In the $n = 3$ level of charmonium there is an overpopulation of states with many missing conventional $\bar{c}c$ states. The first challenge in this level is the identification of the 3^3S_1 charmonium state (the $\psi(3S)$). The calculation of the mass of this state requires the complete numerical analysis of Eq. (146) which is beyond the scope of this paper. However, modulo corrections of order α_s^4, the Bohr scale can be obtained from two successive Bohr levels, e.g. from the $2S$ and $1S$ bottomonium states we get

$$\mu_B(m_b) \approx \frac{M[\Upsilon(2S)] - M[\Upsilon(1S)]}{\epsilon_{20}(\lambda_b) - \epsilon_{10}(\lambda_b)} = 343\ MeV. \tag{167}$$

Similar values are obtained using the $3S$ and $2S$ levels

$$\mu_B(m_b) \approx \frac{M[\Upsilon(3S)] - M[\Upsilon(2S)]}{\epsilon_{30}(\lambda_b) - \epsilon_{20}(\lambda_b)} = 350\ MeV. \tag{168}$$

For the charmonium Bohr scale we get

$$\mu_B(m_c) \approx \frac{M[\psi(2S)] - M[J/\psi(1S)]}{\epsilon_{20}(\lambda_c) - \epsilon_{10}(\lambda_c)} = 319 \ MeV. \tag{169}$$

We can use this value to estimate the mass of the $\psi(3S)$ state as

$$M[\psi(3S)] \approx M[\psi(2S)] + \mu_B(m_c)(\epsilon_{30}(\lambda_c) - \epsilon_{20}(\lambda_c)) = 4041 \ MeV. \tag{170}$$

We expect order α_s^4 corrections to these results, meaning corrections of the order of $\mu_f(m_c) = 18.37 \ MeV$. Notice that the only ψ state above the $\psi(2S)$ in Table III which is consistent with these values is the $\psi(4040)$. We conclude that the $\psi(4040)$ is the 3^3S_1 charmonium state. This conclusion is reinforced by the fact that the mass of the 3^3P_2 (the $\chi_{c2}(3930)$) state is below the mass of the 3^3S_1 state as required by the inverted spectrum of the Cornell potential.

The identification of the $\psi(4040)$ as the $\psi(3S)$ charmonium state, has the interesting prediction that all the $^3S_1$ states lying below the $\psi(4040)$ and above the $\psi(2S)$ states, i.e. the $\psi(3770)$, $\psi(3823)$ and $\psi(3842)$, are not $\bar{c}c$ states (see the review [32] for proposals for the non $\bar{c}c$ nature of some of these mesons).

Once we identify the $\psi(4040)$ as the $\psi(3S)$ charmonium state, we are able to predict the mass of the 3^1S_0 charmonium state (the $\eta_c(3S)$) which according to Eq. (150) must have a mass

$$M[\eta_c(3S)] = M[\psi(3S)] - \mu_f(m_c)f_{30}^{ss}(\lambda_c) = 4003 \pm 4 \ MeV. \tag{171}$$

According to the inverted spectrum obtained with the complete analytical solution of the Cornell potential, the $n = 3$, P-wave states must lie below the $\psi(3S)$ and the $\eta_c(3S)$. This pattern requires the $\chi_{c2}(3930)$ to be the $\chi_{c2}(2P)$ state. The remaining P-waves must lie below the $\chi_{c2}(3930)$ and it is not likely that the $\chi_{c0}(3915)$ be a $\bar{c}c$ state because it is too close to the $\chi_{c2}(3930)$. However, rigourous statements on the identification of the $n = 3$ P-wave charmonium states with the measured $\chi_{c0}(3915)$, $\chi_{c1}(3872)$ and on the missing $h_c(2P)$ requires to do the complete numerical analysis of our main result in Eq. (146). Similarly, the missing $n = 3$ D-waves must be below the P-waves but no definitive statements can be done on the masses of these states until a complete numerical analysis of the fine structure effects in the $n = 3$ level is done. The inverted spectrum of the Cornell potential however, requires that all these states lie between the $\psi(2S)$ and the $\chi_{c2}(3930)$ i.e. in the $[3686, 3925] \ MeV$ energy range, with P-wave states being heavier than the D-wave states. Our analysis of the leading fine splittings requires in turn that the masses of these states be ordered according to Eqs. (155,156).

VI. CONCLUSIONS AND PERSPECTIVES

In this work we completely solve the Cornel potential using the supersymmetric expansion algorithm introduced in Ref. [34]. The solutions are obtained in the form of power series in the normalized string tension λ. Although the power series have a small convergence radius, the actual value of the energy functions $E_{nl}(\lambda)$ and of the radial solutions $R_{nl}(r, \lambda)$ can be reconstructed from the power series using Padé approximants. This reconstruction gets more faithful as we increase the number of terms calculated in the power series. For the purposes of this work we wrote a Mathematica symbolic code, freely available upon request, to calculate the power series to order λ^{301}.

The first main result of the complete analytical solution obtained in this work is the prediction of an *inverted spectrum* for the Cornell potential. This means that energy levels depend on two quantum numbers, the principal quantum number n and the orbital quantum number l, this dependence being actually a function of n^2 and $L^2 \equiv l(l+1)$, and for a given n the energy levels *decrease* with increasing l. The radial probabilities have the same shape as the Coulomb ones but the peaks are shifted to smaller radius, thus Cornell eigenstates are more compact than Coulomb eigenstates.

We calculate the critical values of λ for each level, defined by $\epsilon_{nl}(\lambda_{cr}) = 0$ for values of n up to $n = 9$. The energy levels exhibit the crossing phenomena starting with the $n = 4$ level where the $\epsilon_{43}(\lambda)$ crosses with the $\epsilon_{30}(\lambda)$ level for $\lambda \approx 0.4$.

We apply this solution to the problem of the calculation of heavy quarkonium properties. The heavy quarkonium masses depend on two well defined energy scales, the perturbative physics scale $\mu_Q = 2m_Q$, the natural scale for the Bohr-like levels $\mu_B = 4m_Q\alpha_s^2/9$, and on the normalized energy solutions $\epsilon_{nl}(\lambda)$. Collecting the masses of all the heavy quarkonium states considered as "well established" by the Particle Data Group we show that the so far measured heavy quarkonium masses exhibit the inverse spectrum pattern predicted by the Cornell potential.

A first estimate of the values of the parameters $\bar{\lambda}_Q, \bar{m}_Q, \bar{\alpha}_s(\bar{m}_Q)$ is extracted considering that the Bohr-like levels correspond to the average values of the physical quarkonium masses for both $Q = b, c$ and using the experimental values for the lowest lying states. Predictions for the highest levels turn out to be slightly above the experimental

values, signaling to the need of relativistic corrections. In spite of this, details of the structure of heavy quarkonium so far missing like the heavy quarkonium radius and the heavy quark squared velocities can be assessed from our solution. We find striking differences in these observables with respect to the Coulomb values. Indeed, a calculation of the inverse mean radius yields a result $\langle nl|(r/a_Q)^{-1}|nl\rangle$ which differ for its Coulomb $1/n^2$ behaviour. The non-perturbative interactions mimicked by the linear term yield smaller radius than the Coulomb interaction for the n levels, which in a given level n increases with the value of the angular momentum l. As to the average squared velocity we find $\langle nl|v^2|nl\rangle = C_{nl}(\lambda)\alpha_s^2$ as expected from NRQCD, but the proportionality constant is large compared with the Coulomb value $C_{nl}(0) = 16/9n^2$ and the non-perturbative effects causes the squared velocity to depend on the orbital quantum number l and to have a value close to $2\alpha_s^2$ for all levels. This result signals to the relevance of relativistic corrections for all the levels of heavy quarkonium, not only for the ground state.

We consider then the leading relativistic corrections and calculate the corresponding fine structure splittings using Rayleigh-Schrödinger perturbation theory. The second main result of this calculation is the expression of the masses of the $n^{2S+1}L_J$ heavy quarkonium states as an expansion in $\alpha_s^2(m_Q)$. Indeed, the formal m_Q^{-2} suppression of the relativistic corrections is actually cancelled by m_Q^2 factor from the involved matrix elements (which include the non-perturbative effects of the linear term) leaving actually a power series in α_s^2. The spectrum involves now three well defined energy scales: The perturbative scale given by $\mu_Q(m_Q) = 2m_Q$, the scale dictating the Bohr-like levels, $\mu_B = \frac{4}{9}m_Q\alpha_s^2(m_Q)$, and the scale of the fine splittings $\mu_f(m_Q) = \frac{64}{243}m_Q\alpha_s^4(m_Q)$. The masses of heavy quarkonium states are given in terms these scales, the normalized energy solutions $\epsilon_{nl}(\lambda)$ and the average values of powers of the heavy quarkonium radius normalized to the Bohr radius a_Q which are dimensionless functions $f^k(\lambda)$ depending only on the normalized string tension λ.

The first general prediction arising from this calculation is that the n^3S_1 states are heavier than the n^1S_0 states. Also, we conclude that the masses of the ^3P_J-wave states have a well defined ordering given by $M[n^3P_2] > M[n^3P_1] > M[n^3P_0]$ for $n = 2, 3$. This ordering is clearly exhibited by the measured states in the $n = 2, 3$ levels of bottomonium and by the measured states in $n = 2$ level of charmonium. Similarly, the masses of the ^3D_J states of heavy quarkonium are predicted to satisfy the following hierarchy: $M[n^3D_3] > M[n^3D_2] > M[n^3D_1]$ for $n = 2, 3$.

A confident extraction of the physical value of the normalized string tension λ_Q for heavy quarkonium is done from data on the fine splittings of the lowest lying $l = 0$ states, finding $\lambda_b = 0.361 \pm 0.054$ and $\lambda_c = 0.482 \pm 0.008$. These values and the obtained solutions allow us to fix the fine splitting heavy quarkonium scales to $\mu_f(m_b) = 10.86 \pm 0.54 \ MeV$ and $\mu_f(m_c) = 18.37 \pm 0.36 \ MeV$. With these values and the obtained normalized probabilities evaluated at the origin, we are able to predict the values of the masses of the $\eta_b(3S)$ and $\eta_b(4S)$ states.

An estimate of the Bohr scales from data of the $n = 1, 2$ S-wave states, in a calculation to order α_s^2, yields $\mu_B(m_b) \approx 335 \ MeV$ and $\mu_B(m_c) \approx 318 \ MeV$. These results allow us to identify the $\psi(4040)$ state as the 3^3S_1 (the $\psi(3S)$) charmonium state and to conclude that the measured $\psi(3770)$, $\psi(3823)$ and $\psi(3842)$, are not $\bar{c}c$ states. In the $n = 3$ P-wave sector we identify the $\chi_{c2}(3930)$ as the 3^3P_2 charmonium state ($\chi_{c2}(2P)$) and conclude that the remaining P-wave states ($h_c(2P), \chi_{c1}(2P), \chi_{c0}(2P)$ and all the D-wave states must lie in the $[3686, 3925] \ MeV$ energy range with the P-wave states being heavier that the D-wave states and the ^3P_J and ^3D_J ordered according to: $M[3^3P_2] > M[3^3P_1] > M[3^3P_0] > M[3^3D_3] > M[3^3D_2] > M[3^3D_1]$.

Finally, this paper yield another interesting application of the supersymmetric expansion algorithm to a long standing unsolved potential of primary importance in the phenomenological description of non-perturbative effects in heavy quarkonium physics. The complete solution of this problem allow us to go from the perturbative to the non-perturbative regime in a controlled manner, revealing and quantifying the role of non-perturbative effects in the conformation of heavy quarkonium. There remain many possibilities for the use of our complete analytical solution to the Cornell potential, including the estimate of fundamental quantities arising in the $NRQCD$ and $pNRQCD$ effective theories and the complete phenomenological analysis of the leading relativistic corrections.

VII. ACKNOWLEDGMENTS

---

[1] E. Eichten, K. Gottfried, T. Kinoshita, J. B. Kogut, K. D. Lane and T.-M. Yan, *The Spectrum of Charmonium*, Phys. Rev. Lett. **34** (1975) 369.

[2] E. Eichten, K. Gottfried, T. Kinoshita, K. D. Lane and T.-M. Yan, *Charmonium: The Model*, *Phys. Rev. D* **17** (1978) 3090.

[3] E. Eichten, K. Gottfried, T. Kinoshita, K. D. Lane and T.-M. Yan, *Charmonium: Comparison with Experiment*, *Phys. Rev. D* **21** (1980) 203.

[4] K. G. Wilson, *Confinement of Quarks*, *Phys. Rev. D* **10** (1974) 2445.

[5] E. Eichten and F. L. Feinberg, *Spin Dependent Forces in Heavy Quark Systems*, *Phys. Rev. Lett.* **43** (1979) 1205.

[6] E. Eichten and F. Feinberg, *Spin Dependent Forces in QCD*, *Phys. Rev. D* **23** (1981) 2724.

[7] W. Buchmuller, *Fine and Hyperfine Structure of Quarkonia*, *Phys. Lett. B* **112** (1982) 479.

[8] D. Gromes, *Relativistic Corrections to the Long Range Quark Anti-quark Potential, Electric Flux Tubes, and Area Law*, *Z. Phys. C* **22** (1984) 265.

[9] D. Gromes, *Spin Dependent Potentials in QCD and the Correct Long Range Spin Orbit Term*, *Z. Phys. C* **26** (1984) 401.

[10] A. Barchielli, E. Montaldi and G. M. Prosperi, *On a Systematic Derivation of the Quark - Anti-quark Potential*, *Nucl. Phys. B* **296** (1988) 625.

[11] A. Barchielli, N. Brambilla and G. M. Prosperi, *Relativistic Corrections to the Quark - anti-Quark Potential and the Quarkonium Spectrum*, *Nuovo Cim. A* **103** (1990) 59.

[12] N. Brambilla and A. Vairo, *Nonperturbative dynamics of the heavy - light quark system in the nonrecoil limit*, *Phys. Lett. B* **407** (1997) 167 [`hep-ph/9703377`].

[13] G. T. Bodwin, E. Braaten and G. P. Lepage, *Rigorous QCD analysis of inclusive annihilation and production of heavy quarkonium*, *Phys. Rev. D* **51** (1995) 1125 [`hep-ph/9407339`].

[14] N. Brambilla, A. Pineda, J. Soto and A. Vairo, *Potential NRQCD: An Effective theory for heavy quarkonium*, *Nucl. Phys. B* **566** (2000) 275 [`hep-ph/9907240`].

[15] Y. Koma, M. Koma and H. Wittig, *Nonperturbative determination of the QCD potential at O(1/m)*, *Phys. Rev. Lett.* **97** (2006) 122003 [`hep-lat/0607009`].

[16] Y. Koma, M. Koma and H. Wittig, *Relativistic corrections to the static potential at O(1/m) and O(1/m**2)*, *PoS* **LATTICE2007** (2007) 111 [`0711.2322`].

[17] C. Quigg and J. L. Rosner, *Quantum Mechanics with Applications to Quarkonium*, *Phys. Rept.* **56** (1979) 167.

[18] W. Lucha, F. F. Schoberl and D. Gromes, *Bound states of quarks*, *Phys. Rept.* **200** (1991) 127.

[19] S. Godfrey and N. Isgur, *Mesons in a Relativized Quark Model with Chromodynamics*, *Phys. Rev. D* **32** (1985) 189.

[20] W. Lucha and F. F. Schoberl, *Solving the Schrodinger equation for bound states with Mathematica 3.0*, *Int. J. Mod. Phys. C* **10** (1999) 607 [`hep-ph/9811453`].

[21] T. Barnes, S. Godfrey and E. S. Swanson, *Higher charmonia*, *Phys. Rev. D* **72** (2005) 054026 [`hep-ph/0505002`].

[22] J.-L. Domenech-Garret and M.-A. Sanchis-Lozano, *Spectroscopy, leptonic decays and the nature of heavy quarkonia*, *Phys. Lett. B* **669** (2008) 52 [`0805.2916`].

[23] B.-Q. Li and K.-T. Chao, *Higher Charmonia and X,Y,Z states with Screened Potential*, *Phys. Rev. D* **79** (2009) 094004 [`0903.5506`].

[24] S. Leitão, A. Stadler, M. T. Peña and E. P. Biernat, *Linear confinement in momentum space: singularity-free bound-state equations*, *Phys. Rev. D* **90** (2014) 096003 [`1408.1834`].

[25] S. Godfrey and K. Moats, *Bottomonium Mesons and Strategies for their Observation*, *Phys. Rev. D* **92** (2015) 054034 [`1507.00024`].

[26] S. Godfrey and K. Moats, *Properties of Excited Charm and Charm-Strange Mesons*, *Phys. Rev. D* **93** (2016) 034035 [`1510.08305`].

[27] W.-J. Deng, H. Liu, L.-C. Gui and X.-H. Zhong, *Charmonium spectrum and their electromagnetic transitions with higher multipole contributions*, *Phys. Rev. D* **95** (2017) 034026 [`1608.00287`].

[28] W.-J. Deng, H. Liu, L.-C. Gui and X.-H. Zhong, *Spectrum and electromagnetic transitions of bottomonium*, *Phys. Rev. D* **95** (2017) 074002 [`1607.04696`].

[29] N. R. Soni, B. R. Joshi, R. P. Shah, H. R. Chauhan and J. N. Pandya, $Q\bar{Q}$ ($Q \in \{b, c\}$) *spectroscopy using the Cornell potential*, *Eur. Phys. J. C* **78** (2018) 592 [`1707.07144`].

[30] V. Mateu, P. G. Ortega, D. R. Entem and F. Fernández, *Calibrating the Naïve Cornell Model with NRQCD*, *Eur. Phys. J. C* **79** (2019) 323 [`1811.01982`].

[31] E. Eichten, S. Godfrey, H. Mahlke and J. L. Rosner, *Quarkonia and their transitions*, *Rev. Mod. Phys.* **80** (2008) 1161 [`hep-ph/0701208`].

[32] N. Brambilla et al., *Heavy Quarkonium: Progress, Puzzles, and Opportunities*, *Eur. Phys. J. C* **71** (2011) 1534 [`1010.5827`].

[33] C. Patrignani, T. K. Pedlar and J. L. Rosner, *Recent Results in Bottomonium*, *Ann. Rev. Nucl. Part. Sci.* **63** (2012) 2008 [`1212.6552`].

[34] M. Napsuciale, S. Rodríguez and M. Kirchbach, *Supersymmetric Expansion Algorithm and Complete Analytical Solution for the Hulthén and Anharmonic Potentials*, *PTEP* **2024** (2024) 083A02 [`2405.01367`].

[35] M. Napsuciale and S. Rodriguez, *Complete analytical solution to the quantum Yukawa potential*, *Phys. Lett. B* **816** (2021) 136218 [`2012.12969`].

[36] M. Napsuciale and S. Rodríguez, *Bound states of the Yukawa potential from hidden supersymmetry*, *PTEP* **2021** (2021) 073B03 [`2102.07160`].

[37] PARTICLE DATA GROUP collaboration, *Review of particle physics*, *Phys. Rev. D* **110** (2024) 030001.

[38] P. Falkensteiner, H. Grosse and F. Schoberl, *RELATIVISTIC CORRECTIONS TO QUARKONIUM SPECTRA*, *Phys. Lett. B* **148** (1984) 194.